GEOCHEMICAL PROPERTIES OF FELDSPARS IN PEGMATITE AND GNEISS ROCKS:

A CASE STUDY OF DAGBALLA, SOUTHERN NIGERIA.

BY

EMMANUEL OSASENAGA IKUOBASE

(PG-PSC1715677)

B.Sc. Geology, UNIBEN.

DEPARTMENT OF GEOLOGY

FACULTY OF PHYSICAL SCIENCES

UNIVERSITY OF BENIN

BENIN CITY, NIGERIA

NOVEMBER, 2021

GEOCHEMICAL PROPERTIES OF FELDSPARS IN PEGMATITE AND GNEISS ROCKS:

A CASE STUDY OF DAGBALLA, SOUTHERN NIGERIA.

BY

EMMANUEL OSASENAGA IKUOBASE

(PG-PSC1715677)

B.Sc. Geology, UNIBEN.

A PROJECT WORK WRITTEN IN THE DEPARTMENT OF GEOLOGY AND SUBMITED TO THE SCHOOL OF POST GRADUATE STUDIES, UNIVERSITY OF BENIN IN PARTIAL FULFILMENT OF THE REQUIREMENT FOR THE AWARD OF MASTERS OF SCIENCE (M.Sc) DEGREE IN GEOLOGY.
(MINERAL EXPLORATION OPTION)

NOVEMBER, 2021

CERTIFICATION

This is to certify that this project was carried out by Mr. Emmanuel Osasenaga Ikuobase of the Department of Geology, University of Benin, Benin City, Edo State, Nigeria.

_____ _____

Professor I.O. Imasuen **Date**
Supervisor

_____ _____

Professor I.O. Imasuen **Date**
Head of Department, Geology

DEDICATION

This project is dedicated to my parents Mr. and Mrs. Victor Ikuobase and siblings Miracle, John and James for consistently encouraging and praying for me during the course of my program in the University of Benin.

ACKNOWLEDGEMENT

I acknowledge the presence of God Almighty in my life, for His wonderful show of love towards me throughout my program.

I wish to acknowledge the immense contribution of the Head of Department Professor I.O. Imasuen who also doubles as my project supervisor for providing a suitable platform and environment during the course of my project presentation.

I also appreciate the special efforts of my lecturers Professor C.N Akujieze, Professor. F.A. Lucas, Dr. Salami, Dr.(Mrs) O. Odokuma-Alonge, Dr. Joel Edegbai, Dr. Alex Ogbamikhumi, Dr. (Mrs) Efe Maju-Oyovwikowhe, Mr. Nosa Igbinigie, Mrs Obayanju for their support and constructive criticism during the course of my project.

To Mr. Daniel Omoruyi, for his supportive role and encouragement during the course of my project preparation.

To my course mates Gbenga, Ezekiel, Ope, Joy, Aladin, Ejike, Omasan, Victoria, Wisdom, Nosa and others whose names are not mentioned, I sincerely appreciate the moments we had together during the duration of this program.

TABLE OF CONTENTS

LIST OF TABLES

LIST OF FIGURES

LIST OF PLATES

ABSTRACT

Ten (10) samples collected from six (06) different locations around Dagballa area in Akoko-Edo area, Southern Nigeria, were studied using field, geochemical and petrographical analysis to determine the relative abundance and distribution of major and minor elements present in the samples. The ten (10) samples comprise nine (09) pegmatite samples and one augen gneiss (01) sample which is the host rock are delineated as DA1-10 for easy recognition. Sampling interval for the rock samples varied depending on the aerial extent of each outcrop and field environmental conditions encountered. DA1 and DA2 were obtained from location 1, DA3 and DA4 from location 2, DA5 and DA6 from location 3, DA7 and DA8 from location 4, DA9 was obtained from location 5 and DA10 was obtained from location 6. The pegmatites in the Dagballa, area occurs as intrusions and is hosted by Augen-Gneiss. There is the presence of a sharp zonation and chilled margin in the first three locations encountered. The estimated contact between the pegmatite and the granite-gneiss is 30m. From thin section analysis, the pegmatites from Dagballa consist of quartz and feldspar minerals with microcline and albite being the dominant feldspar minerals present in most of the samples. Also, muscovite, biotite, opaque and other accessory minerals are present in minute quantities. Composite whole-rock samples were analyzed for major and minor oxides using X-Ray Fluorescence Spectrometer (XRF). The results reveal the pegmatites are very siliceous with SiO_2 values of 66.75 wt.% to 74.75 wt.%. Al_2O_3 values are relatively moderate between14.57 wt.% to 15.61 wt.%. Na_2O and K_2O abundances are low and ranges between 2.76 wt.% to 5.56 wt.% and 3.50 wt.% to 8.43 wt.% respectively. MgO abundances are generally low (0.05-0.20 wt.%). Fe_2O_3 abundances are generally low between 0.30-0.47 wt.% with the exception been the abundance (5.82 wt.%) probably obtained from the host rock. Alumina saturation index (A/CNK) computation with values ranging from 1.160 to 1.738 indicates the rock samples are all peraluminous and therefore indicate S-type granite.

CHAPTER ONE

INTORDUCTION

1.1 GENERAL STATEMENT

Dagballa is situated within the Igarra Schist Belt of the Nigeria Basement Complex. The Dagballa area lies within Latitudes $07^{\circ}\ 19^{1}\ 30^{11}$N- $07^{\circ}\ 21^{1}\ 0^{11}$N and Longitudes $006^{\circ}\ 12^{1}\ 30^{11}$E-$006^{\circ}\ 14^{1}\ 0^{11}$E. The major rock found in this area is the Augen Gneiss (NGSA, 2015). The host rock (augen gneiss) is intruded by pegmatites which occur as dykes. The pegmatites and augen gneiss host a considerable amount of feldspar minerals which are the main point of interest of this study.

1.2 GEOCHEMISTRY OF FELDSPAR

Feldspar is the name given to a large group of rock-forming silicate minerals that constitute more than 50% of the earth's crust (Hobart, 2015). They are found in igneous, metamorphic and sedimentary rocks in all parts of the world. Feldspar minerals have very similar structures, chemical compositions, and physical properties. The common feldspar minerals include orthoclase, albite and anorthite. Feldspar minerals have many uses in industry; they are widely used in the manufacture of a wide variety of glass and ceramic products. They are also often used as fillers in paints, plastics and rubber. Some of the most popular gemstones are feldspar minerals.

1.2.1 FELDSPAR MINERAL CHEMISTRY

All of the minerals in the feldspar group can be fit into a generalized chemical composition: $X(Al,Si)_4O_8$. In the generalized composition, any one of the following seven ions: K^{+}, Na^{+}, Ca^{++}, Ba^{++}, Rb^{++}, Sr^{++}, and Fe^{++} can be used in substitution for X. Feldspars containing potassium, sodium and calcium ions are very common. Barium, rubidium, strontium and iron feldspars are very scarce. The triangular diagram in Figure 1 shows two solid solution systems that comprise the feldspar group. The plagioclase feldspars form a solid solution series between the end members of pure albite ($NaAlSiO_8$) and pure anorthite ($CaAl_2Si_2O_8$). The alkali feldspars form a solid solution series between pure albite and potassium sanidine ($KAlSi_3O_8$). Table 1 shows a list

of the plagioclase feldspars in variation with the composition of albite and anorthite present in them.

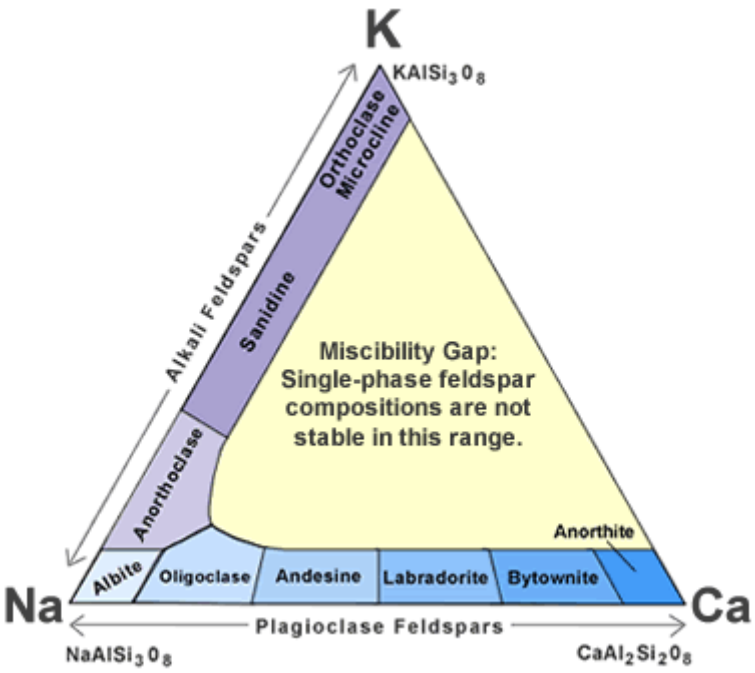

Figure 1: A Tenary Diagram Showing Feldpar Classification (Dyar and Gunter 2008)

Table 1: List of Feldspar Minerals with their Chemical Compositions (Hobart, 2015)

Plagioclase Mineral Name	Percent NaAlSiO3O8	Percent CaAl2Si2O8
Albite	100-90% albite	0-10% anorthite
Oligoclase	90-70% albite	10-30% anorthite
Andesine	70-50% albite	30-50% anorthite
Labradorite	50-30% albite	50-70% anorthite
Bytownite	30-10% albite	70-90% anorthite
Anorthite	10-0% albite	90-100% anorhtite

1.2.2 THE PLAGIOCLASE FELDSPAR

Albite and anorthite which are sodium and calcium feldspar, respectively, form through crystallization from a melt. Due to the abundance of sodium, calcium, aluminium, silicon and oxygen present in melts, most albite will contain some calcium substituting for sodium in its crystalline structure, and most anorthite will contain some substitution of sodium for calcium in its crystalline structure. As a result, if a sodium ion with a +1 charge substitutes for a calcium ion with a +2 charge, a balancing substitution of an aluminium ion with a +3 charge for a silicon ion with a +4 charge will also occur (Hobart, 2015).

The relative abundance of sodium and calcium in melts varies greatly, and the whole range of mineral compositions between pure sodium plagioclase and pure calcium plagioclase occurs. This process of continuum is known as a solid solution series because it is similar to melt containing dissolved sodium and calcium ions suspended in different positions in the solution and is referred to as a melt (Hobart, 2015).

Also, the range of mineral compositions, from pure albite and pure anorthite is made up of very similar minerals, but there are differences in their chemical and physical properties. In order to make communication easier, names are given to the feldspar minerals in a variety of positions in the plagioclase solid solution (Hobart, 2015). These names are arbitrary and are based upon the relative amounts of albite and anorthite in their composition. The names of these plagioclase minerals of intermediate compositions are summarized in Table 2. They can also be seen forming the plagioclase feldspar series along the base of the triangular diagram described above.

Table 2: Many Types of Feldspar (Hobart, 2015)

Mineral	Composition
Albite	$NaAlSi_3O_8$
Amazonite	$KAlSi_3O_8$
Andesine	$(Na,Ca)(Al,Si)_4O_8$
Anorthite	$CaAl_2Si_2O_8$
Anorthoclase	$(Na,K)AlSi_3O_8$
Banalsite	$Na_2BaAl_4Si_4O_{16}$
Buddingtonite	$(NH_4)AlSi_3O_8$
Bytownite	$(Ca,Na)(Al,Si)_4O_8$
Celsian	$BaAl_2Si_2O_8$
Dmisteinbergite	$CaAl_2Si_2O_8$
Filatovite	$K(Al,Zn)_2(As,Si)_2O_8$
Hexacelsian	$BaAl_2Si_2O_8$
Hyalophane	$(K,Ba)(Al,Si)_4O_8$
Kokchetavite	$KAlSi_3O_8$
Kumdykolite	$NaAlSi_3O_8$
Labradorite	$(Ca,Na)(Al,Si)_4O_8$
Microcline	$KAlSi_3O_8$
Oligoclase	$(Na,Ca)(Al,Si)_4O_8$
Orthoclase	$KAlSi_3O_8$
Paracelsian	$BaAl_2Si_2O_8$
Reedmergnerite	$NaBSi_3O_8$
Rubicline	$(Rb,K)AlSi_3O_8$
Sanidine	$KAlSi_3O_8$
Slawsonite	$SrAl_2Si_2O_8$
Stronalsite	$Na_2SrAl_4Si_4O_{16}$
Svyatoslavite	$CaAl_2Si_2O_8$

1.2.3 THE ALKALI FELDSPARS

Feldspar minerals with compositions that range between $NaAlSi_3O_8$ and $KAlSi_3O_8$ are generally known as alkali feldspars (Hobart, 2015). They include albite ($NaAlSi_3O_8$), anorthoclase ($(Na,K)AlSi_3O_8$), sanidine [$(K,Na)AlSi_3O_8$], orthoclase ($KAlSi_3O_8$), and microcline ($KAlSi_3O_8$). Albite and sanidine form a solid solution series between $NaAlSi_3O_8$ and $KAlSi_3O_8$. Anorthoclase, with a composition of $(Na,K)AlSi_3O_8$, occupies the intermediate position between them (Hobart, 2015).

Orthoclase and microcline usually have compositions that are very close to $KAlSi_3O_8$. Sanidine can also have a composition very close to $KAlSi_3O_8$. These three $KAlSi_3O_8$ minerals are polymorphs, meaning they are made of the same chemical compositions but different crystal structures. Sanidine and orthoclase has a monoclinic structure, and microcline is triclinic. Temperature is a major factor in the formation of these three minerals with a $KAlSi_3O_8$ composition. Sanidine is the high-temperature form, orthoclase is the intermediate-temperature form, and microcline is the low-temperature form. Figure 2 shows that feldspar minerals are important constituents of granite, diorite and gabbro- these rock types make up the majority of Earth's crust. Figure 3 shows the right-angle cleavage displayed by the feldspar minerals. Table 3 shows the physical properties of feldspar minerals and their uses.

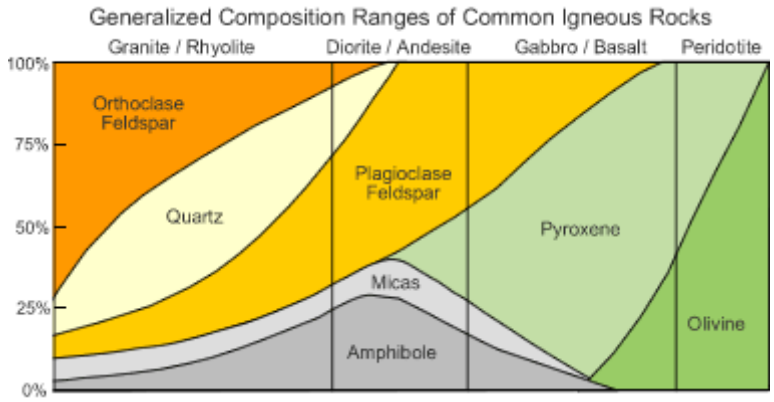

Figure 2: Mineral Compositions of Common Igneous Rocks (Hobart, 2015)

Fig 3: Right-Angle Feldspar Cleavage (Hobart, 2015)

Table 3: Generalized Physical Properties of Feldspar Minerals (Hobart, 2015)

PROPERTIES	DESCRIPTION
Colour	Usually white, pink, gray or brown. Also colorless, yellow, orange, red, black, blue, green.
Streak	White
Luster	Vitreous, Pearly on some cleavage faces.
Diaphaneity	Usually translucent to opaque. Rarely transparent.
Cleavage	Perfect in two directions. Cleavage planes usually intersect at or close to a 90 degree angle.
Mohs Hardness	6 to 6.5
Specific Gravity	2.5 to 2.8
Diagnostic Properties	Perfect cleavage, with cleavage faces usually intersecting at or close to 90 degrees. Consistent hardness, specific gravity and pearly luster on cleavage faces.
Chemical Composition	A generalized chemical composition of $X(Al,Si)_4O_8$, where X is usually potassium, sodium, or calcium, but rarely can be barium, rubidium, or strontium
Crystal System	Triclinic, monoclinic
Uses	Crushed and powdered feldspar are important raw materials for the manufacture of plate glass, container glass, ceramic products, paints, plastics and many other products. Varieties of orthoclase, labradorite, oligoclase, microcline and other feldspar minerals have been cut and used as faceted and cabochon gems.

1.3 PEGMATITES

A Pegmatite is a type of igneous rock which is formed by slow crystallization at high temperature and pressure at depths and exhibiting large interlocking crystals usually greater in size than 2.5cm (Winter, 2014). Pegmatites are texturally distinct variants of the more common and more voluminous plutonic igneous rocks, including Gabbros, Granites, Syenites, etc. Most Pegmatite bodies are small with dimensions on the scale of meters rather than kilometers, and display internally complex fabrics.

The mineralogy and texture of Pegmatites tend to be heterogeneous over a large volume of rocks. The composition of pegmatite is similar to Granite and they are composed mainly of quartz, feldspar and mica. The crystals of quartz and feldspars present in Pegmatites are intertwined, ranging several centimeters up to tens of meters in length and they are usually coarse-grained and crystalline. Other rare Pegmatites found in recrystallized zones and apophyses associated with large layered intrusions contain intermediate and mafic minerals such as amphibole, Ca-plagioclase feldspar, pyroxene and feldspathoids. Feldspar within a Pegmatite may display exaggerated and perfect twinning, ex-solution lamellae, and when affected by hydrous crystallization, macro-scale graphic texture is known, with feldspar and quartz inter-grown. Perthite feldspar within a pegmatite often shows gigantic perthitic texture visible to the naked eye. The product of Pegmatite decomposition is Euclase.

Pegmatites usually occur as segregations within granites and as sharply discordant dikes intruding igneous and metamorphic rocks (London and Kontak, 2012).

Pegmatites occur throughout the Basement Complex of Nigeria. There are numerous studies on these Pegmatites. Earlier study of Pegmatites in Nigeria includes the work of Jacobson and Webb (1946), Garba (2003), Okunlola and Akintola (2008), Muhammad (2014), Suleiman (2016), Omoruyi and Imeokparia (2021).

1.3.1 Features that distinguish Pegmatites from other Plutonic Igneous Rocks

- Large crystal size.
- Systematic coarsening in crystal size from the margins to the center of the bodies.
- Sharp mineralogical zonation from margin to center.
- Anisotropic fabrics including layering or highly oriented crystal growth directions.
- Graphic (skeletal) intergrowths of quartz and feldspar, termed “graphite granite”.

Pegmatites and hydrothermal vein deposits share all of these textural features except the graphic intergrowths of quartz and feldspar present in Pegmatites.

Pegmatitic textures can be found in igneous rocks of all compositions. However, pegmatitic textures are so prevalent in granitic compositions that the term pegmatite implies a granitic composition to many geoscientists (London and Kontak, 2012).

1.3.2 Pegmatites as Ore Bodies

Pegmatites host an exceptionally diverse range of economic commodities. The unique textural characteristics of Pegmatites makes it possible for the concentration of trace elements as chemically diverse as Li, B, Cs, Ta and Bi to values that are thousands of times there average crustal abundances (Hobart, 2015). Element pairs that behave in a chemically coherent fashion, for example Zr-Hf and Nb-Ta, are extensively fractionated among Pegmatites and within individual bodies, leading to the formation of such exotic mineral species as hafnon ($HfSiO_4$) and tantite (Ta_2O_5) (London and Kontak, 2012). The process of rare-element enrichment in Pegmatites appears to proceed, in an essentially closed system, from a small fraction of residual silicate liquid derived from a much large magma body (London and Kontak, 2012). This process contrasts markedly with other ore-forming systems, for example Cu-and Mo-mineralized felsic porphyries, that originate from inter-actions between large volumes of magmatic rocks and hydrothermal fluids in chemically open systems.

1.3.3 Pegmatites as Storehouses of Industrial Minerals

Pegmatites are the primary sources of feldspar for glass and ceramics industries. Quartz is used primarily in the manufacture of glasses, but ultra-high-purity quartz from pegmatite is a foundational material in the electronics industry. Because Pegmatites consist mainly of quartz and feldspars, the ore grade of some of the most important deposits approaches 100% of the minable rock, a benefit that is rare in the mining industry.

1.4 GNEISS

Gneiss is a foliated metamorphic rock identified by its bands and lenses of varying mineral composition. Some of these bands contain granular minerals that are bound together in an interlocking texture (Bucher and Grapes, 2011). Other bands contain platy or elongated minerals that show a preferred orientation that is parallel to the overall banding in the rock. It is this banded appearance and texture rather than composition that defines a Gneiss (Vernon, 2018).

1.4.1 Formation of Gneiss

Gneiss usually forms by regional metamorphism at convergent plate boundaries. It is a high-grade metamorphic rock in which mineral grains recrystallized under intense heat and pressure (Bucher and Grapes, 2011). This alteration increases the size of the mineral grains and segregate them into bands, a transformation which makes the rock and its minerals more stable in their metamorphic environment. During this transformation, clay particles in Shale transformed into micas, begin to recrystallize into granular minerals. The appearance of granular minerals is what marks the transition into Gneiss (Bucher and Grapes, 2011). Intense heat and pressure can also metamorphose Granite into a banded rock known as “Granite-Gneiss”. This transformation is usually more of a structural change than a mineralogical transformation (Shelley, 1993).

1.4.2 Composition and Texture of Gneiss

Most specimens have bands of feldspar and quartz grains in an interlocking texture. These bands are usually light in colors and alternate with bands of darker-colored minerals with platy or elongate habits. The dark minerals sometimes exhibit an orientation determined by the pressure of metamorphism (Shelley, 1993). Some specimens of Gneiss contain distinctive minerals characteristic of the metamorphic environment. These minerals might include Biotite, Cordierite, Sillimanite, Staurolite, Andalusite and Garnet (Vernon and Clarke, 2008).

1.4.3 AUGEN GNEISS

Augen gneiss is a coarse grained gneiss resulting from metamorphism of granite which contains characteristic elliptic or lenticular shear-bound grains feldspar (porphyroclasts), normally microcline, surrounded by finer grained material (Bucher and Grapes, 2011). The finer grained material deforms around the more resistant feldspar grains to produce this texture or within the layering of the quartz, biotite and magnetite bands (Vernon and Clarke, 2008).

1.5 AIM AND OBJECTIVES OF THE STUDY

This research project is aimed at studying the geochemistry of feldspars present in pegmatitic rocks of the Igarra Schist Belt. Therefore the scope of the research involves comprehensive geological, structural and geochemical study of the Igarra Schist belt, with a view to:

a) Produce a detailed geological map of the study area on a scale of 1:30,000.
b) Undertake petrographic microscopic study of the component rock types.
c) Provide mineral and chemical data through geochemical analyses of representative samples that are systematically collected from the area.
d) Determine some statistical analyses on the sample to find out the relationships between the major oxides present in the component rock types.
e) To qualify the pegmatites present in Dagballa.

1.6 SCOPE OF THE STUDY

- Library review of works to locate Pegmatite occurrences in study areas.
- Field work which entails detail mapping and sampling of the Pegmatite bodies.
- Laboratory sample preparation for petrographic and geochemical studies of the Pegmatites.
- Instrumental sample analyses using petrographic microscope and X-ray Fluorescence.
- Data interpretation.

1.7 LOCATION AND ACCESSIBILITY OF THE STUDY AREA

Igarra is the headquarters of Akoko-Edo Local Government Area of Edo State, Nigeria. It is located at Latitudes $07^{\circ}14^{1}$N-$07^{\circ}37^{1}$N and Longitudes $006^{\circ}00^{1}$-$006^{\circ}30^{1}$ in the northern outskirts of Edo State. The area of study, Dagballa is located in Akoko-Edo Local Government and it lies within Latitude $07^{\circ}20^{1}$N and Longitude $006^{\circ}13^{1}$E. Igarra is located in the northern part of Edo State and it is underlain in the north by Precambrian Basement Complex and in the south by Cretaceous and Tertiary sediments.

The major highway in the area of study starts from Auchi through, Sobe-Ogbe, Ikpeshi, Igarra to Ibillo. There are also other major footpaths which are indicated in the accessibility map. The coordinates of the sample locations are shown in Table 4. Figure 5 shows the various locations visited in Dangballa.

Table 4: Different Locations with their Coordinates

Location	Northings	Eastings	Elevation	Dip direction	Strike
1	07° 20¹ 08.3¹¹	006° 13¹ 13.1¹¹	337m	280°NW	NORTH-SOUTH
2	07° 19¹ 54.2¹¹	006° 13¹ 07¹¹	357m		
3	07° 19¹ 40¹¹	006° 13¹ 10¹¹	358m		
4	07° 20¹ 49¹¹	006° 13¹ 09¹¹	349m		EAST-WEST
5	07° 20¹ 54¹¹	006° 13¹ 00¹¹	343m		
6	07° 20¹ 58¹¹	006° 12¹ 55¹¹	338m		

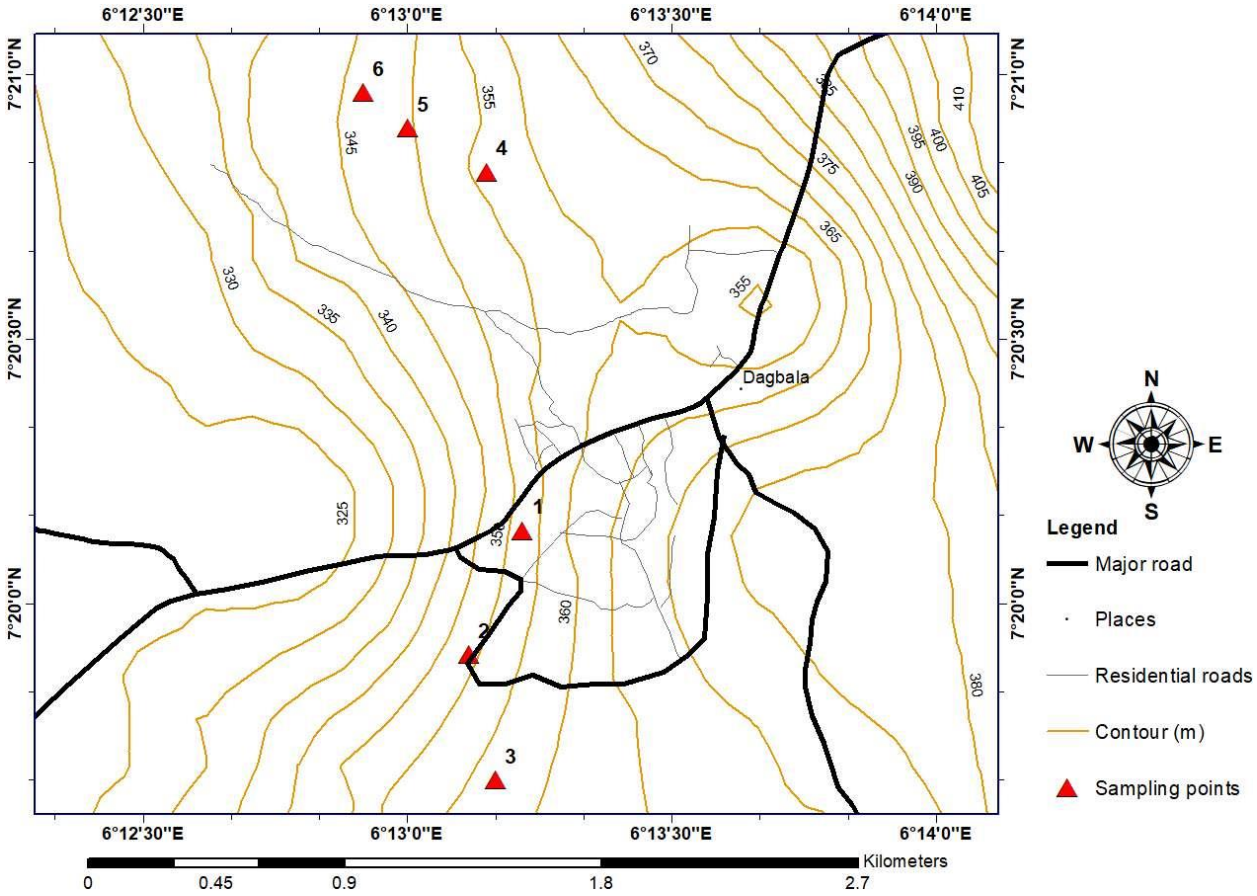

Figure 4: Location Map of Study Area with Sample Locations

1.8 TOPOGRAPHY AND DRAINAGE OF STUDY AREA

The topographic of the study area is influenced by the underlying geology (I.I Obiadi *et al*, 2015). It is characterized by highland especially the tall ranking older granite suites adjacent to the relatively low lying plains (essentially the weathered schist belt). The area is drained by a system of rivers and streams, flowing generally in the North-South direction. The stream channels are nearly parallel to the strike of the Schistose rocks suggesting they are structurally controlled.

1.9 CLIMATE AND VEGETATION OF STUDY AREA

Igarra and its environs fall within the warm-humid tropical climate region were the rainy and dry seasons are noticed mainly in the area. The rainy season last for about seven months i.e. between May to October and the dry season last for about five months i.e. between November to April. The rainfall is moderate, between the months of March and May and falls heavily between June and September with an average rainfall between 1000mm and 1500mm and the temperature is as high as 36.7°C especially during the hottest period of February to April (Ademila *et al*, 2019).

The study area is located in the Guinea Savannah vegetation belt which is characterized by short tress and tall grasses. Humidity in the area is constantly high, and the area enjoys adequate rainfall. The exercise took place over the course of the dry season and as a result, the weather was hot and dry in the morning, and sunny in the afternoon (Oloto and Anyanwu, 2013).

In addition, the study area lies in the transition between tropical rain forest and savannah (grassland). As a result, the vegetation cover of the region is made up of the wooded area belt (which consists of the central and southern part of the state) and the Guinea Savannah (which consists of the northern part of the state where the study area is located). The vegetation here is mainly as a result of sparsely distributed trees, herbs, shrubs, and grasses. The trees help to control soil erosion (Oloto and Anyanwu, 2013).

CHAPTER TWO

LITERATURE REVIEW

2.1 THE BASEMENT COMPLEX OF NIGERIA

The Basement Complex of Nigeria lies in a vast area east of the West African Craton that was subjected to the Pan-African orogenic event about 600 Ma ago. Evidence from Hogar (Pharusian), Ghana and Togo indicates that this belt evolved through plate tectonic activities involving collision and subduction resulting in the partial melting of the lower crust and formation of granitic magma leading to the emplacement of the Older Granites (Ajibade and Wright, 1989).

Within the basement are domains of Metasedimentary, Metavolcanics and intrusive igneous rocks which constitute the north-south trending schist belts. They are considered to be Upper Proterozoic assemblages that lie on the migmatites-gneisses-quartzite complex (Turner, 1983). The Schist Belts which are concentrated in the western half of Nigeria are seldom found east of 8◦E longitude (Ajibade and Wright, 1989; Akintola and Adekeye, 2008). They host most of the economic minerals in the basement complex (Akande and Kinnaird, 1990). The following rock groups are recognized in the Nigerian Basement Complex;

I. Polycyclic migmatites-gneiss-quartzite complex (Rahaman, 1988; Dada, 2006)
II. Schist belts composed of metasedimentary and metavolcanics (Rahaman, 1981; Egbuniwe, 1982; Turner, 1983)
III. Older Granites (Falconer, 1911; Rahaman, 1981; Rahaman, 1988; Dada, 2006) and
IV. Minor Felsic and minor intrusive (Dada, 2006).

2.1.1 THE MIGMATITES-GNEISS-QUARTZITE COMPLEX

The Migmatites-Gneiss-Quartzite Complex is high grade metamorphic rocks of various compositions which are believed to account for about 60% of the basement rocks of Nigeria (Rahaman *et al*., 1988). They usually comprise of Migmatite and Gneiss of various composition

and structures. Metamorphism is generally in the Amphibolites to granulite facie grade. Associated with these are relicts of ancient metasediments (commonly feldspathic quartzites) which were correlated with the Birrimian Metasediments of Ghana (McCurry, 1976). The Gneisses and Migmatites are so initimately associated such that they are hardly separated in the field. They are commonly seen and from the bulk of the rocks in this group. Banding of various widths is the common feature or structure displayed by these rocks.

According to Dada (1997), there was crustal addition in the crystalline basement complex of Nigeria that occur about 3500 Ma. Dada obtained ages greater than 3000 Ma from some of the Basement Rocks as shown in a geochronology for the Basement Rocks of Nigeria modified by Dada (1997) after McCurry (1976) as shown in Table 5. Age determination across the country shows that the Migmatite-Gneiss complex contains rocks that are as old as 3000 Ma and those as young as 600 Ma as shown in Table 5.

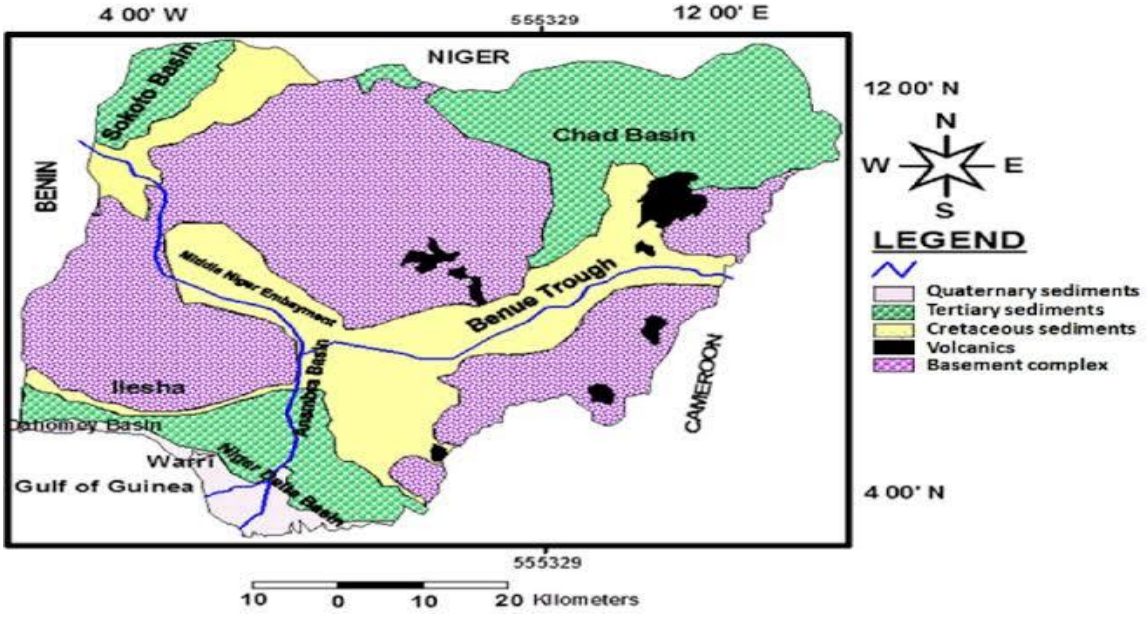

Fig 5: Geologic Map of Nigeria, Indicating the Basement Complex (Bankole, 2016)

Table 5: A Generalized Geochronology for The Basement Rocks Of Nigeria (Modified After Mccurry, 1976; Dada 1997).

Age (Ma)	Period (or epoch)	Activity	Remarks
540± 40	Late Pan-African	Uplift, cooling, faulting, high level magmatic activities	
650-580	Pan-African	Granitic intrusion, pegmatites and aplite development	Older Granites Magmatism
650-850	(Main Phase)	Orogenesis: deformation, metamorphism, migmatisation and reactivation of pre-existing rocks.	
800-1000	Katinga	Geosynclinal deposition, intrusion of hypersthenes-bearing rocks.	Katangan Metasediments
1900±250	Eburnean	Granitic intrusion Orogenesis: folding, metamorphism and reactivation of pre-existing rocks.	Eburnean granites
2500	Birrimian	Geosynclinal deposition	Birrimian metasediments
3100-2750 Dada (1997)		Orogenesis and metamorphism	Emplacement of granodioritic magama
3500 Dada (1997)		Crystalline basement	Crustal addition

2.1.2 SCHISTS BELTS

The Schist Belts form approximately north to south trending narrow zones of low to medium grade metamorphic rocks of mainly sedimentary and minor igneous origin, which were deposited previously on the pre-existing Migmatite-Gneiss-Quartzite Complex. The rocks of the belt are also described as 'Younger Metasediments' composed of Phyllite, Schist Quartzite, Amphibolites and flaggy gneiss of Paleo-Protezoic age (Akande and Kinnaird, 1990). Other secondary rocks used in delineating them are Carbonates, Calc-Gneiss and Banded Iron Formation (BIF). Metamorphism within the Schist Belts is predominantly of the Greenschist Facies grading into the Amphibolites Facies, especially in the older Migmatite-Gneiss-Quartzite Complex (Akande and Kinnaird, 1990).

Structurally, two major transcurrent fault systems fault systems with dextral displacement are known in the Precambrian Basement. They trend in the NE-SW direction displacing earlier structures in the order of tens of kilometers. The two fault systems are the Anka fault and the Kalangai fault and are often associated with locally developed subsidiary (NW-SE) sinistral fault and are considered to be conjugate system of late Pan-African brittle deformation that occurred after about 530 Ma on a continental scale (Ball, 1980; Danbatta, 2003).

2.1.3 THE OLDER GRANITES

The Older Granites intrude the Migmatite-Gneiss Complex and low grade Schist Belts. In general, the Older Granites range in size from sub-elliptical plutons to elongated Batholiths up to 60km. The bodies are usually elongated parallel to the regional trend and may be foliated. Foliation when present is also parallel to that of the country rocks. The Older Granites vary in composition from true granites to granodiorites and tonalities. They also vary in texture from fine grained to coarse grained porphyritic granites rocks. However, the medium to coarse-grained porphyritic variety is more common. Other rock types which normally occur in association with granitic rocks include Charnockite, Gabbro, and Syenite.

Field relations show that Older Granites are composite bodies, usually composed of two or more intrusions.

2.1.4 MINOR FELSIC AND MAFIC INTRUSIVES

The Minor Felsic and Mafic Intrusives consist of concordant and discorcordant dykes, veins and irregular bodies of Pegmatite, Aplite, Quartz, Dolerite, Gabbro, Pyroxenite and Serpentinite. As the youngest members of the Basement Complex of Nigeria, rocks of these units intruded almost all the pre-existing rocks. The Pegmatite host tourmaline and beryl gemstone, tantalite, columbite and cassiterite. They also contain feldspars and micas in exploitable quantities.

2.2 LITERATURE REVIEW OF IGARRA SCHIST-BELT

The Nigerian Schist belts are a part of the Basement Complex, which is composed of other rock suites, such as the migmatite-gneiss complex, which has been intruded by Pan-African Granite. The Meta-sediments, acting as a supra-crustal lid on the top of the basement, consisting of quartzites, meta-conglomerate, and mica-schist and marble (Okeke and Meju, 1985; Ajibade et al., 1987; Imeokparia, and Emofurieta, 1991). The Igarra in the meta-sedimentary belt is one of the most prominent Slate Belt, which is located in the south-western part of Nigeria). The Slate Belt acts as a N-S trending zone of low-to-medium grade meta-sediments, such as Phyllite, and semi-pelitic to pelitic Schist, meta-greywacke, meta-conglomerates, quartzites, and basic to ultrabasic metavolcanics (Rahaman, 1988; McCurry, 1989; Annor, 1998).

Odeyemi (1976), classified the basement around Igarra into three groups, namely: the Migmatite-Gneiss Complex, low grade meta-sediments and Granitoids. Apart from the intrusive rocks, the foliation exhibited by the basement rocks of Southwestern Nigeria is of tectonic origin (Odeyemi, 1988).

According to Boesse and Ocan (1992), the Igarra Schist belt has experienced two phases of orogeny (deformation); the first phase (D1) produced tight to isoclinal folds with north-southerly direction while the second phase (D2) that was characterized by more open folds of variable style with large vertical NNE-SSW trending fault. Fractures ranging from minor (joints) to major ones were ubiquitous among the meta-sediments and the intrusives, some of which were filled by quartz veins trending generally in NE-SW direction.

The age of the Igarra Schist belt has been debated by different scholars, but Ogezi (1977) obtained a Neoproterozoic (Pan-African) and this age was affirmed by Ajibade et al. (1989). This age was interpreted as too young to represent the age of metamorphism but instead reflects a later heating event related to the Older Granite activity during the Pan-African (Annor, 1988). Paleoproterozoic age was also suggested by Olobaniyi (2003) based on the close association of the Schist of the Isanlu area (Egbe-Isanlu Schist belt) with Talc Schist and Banded Iron Formation that are regarded as markers for the early Precambrian.

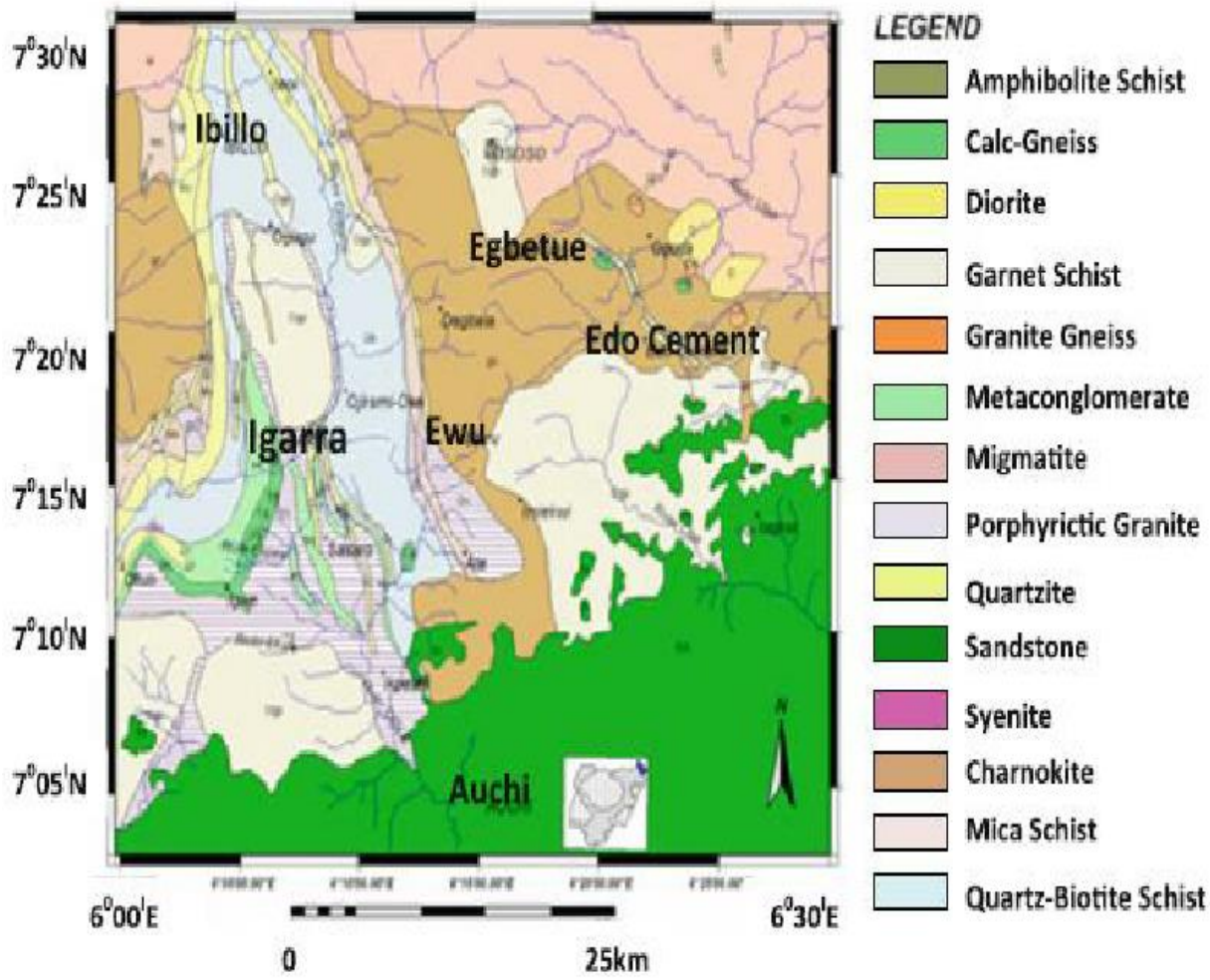

Fig 6: Geologic Map Showing the different lithologies in the Igarra Schist Belt (Obiadi et al., 2015)

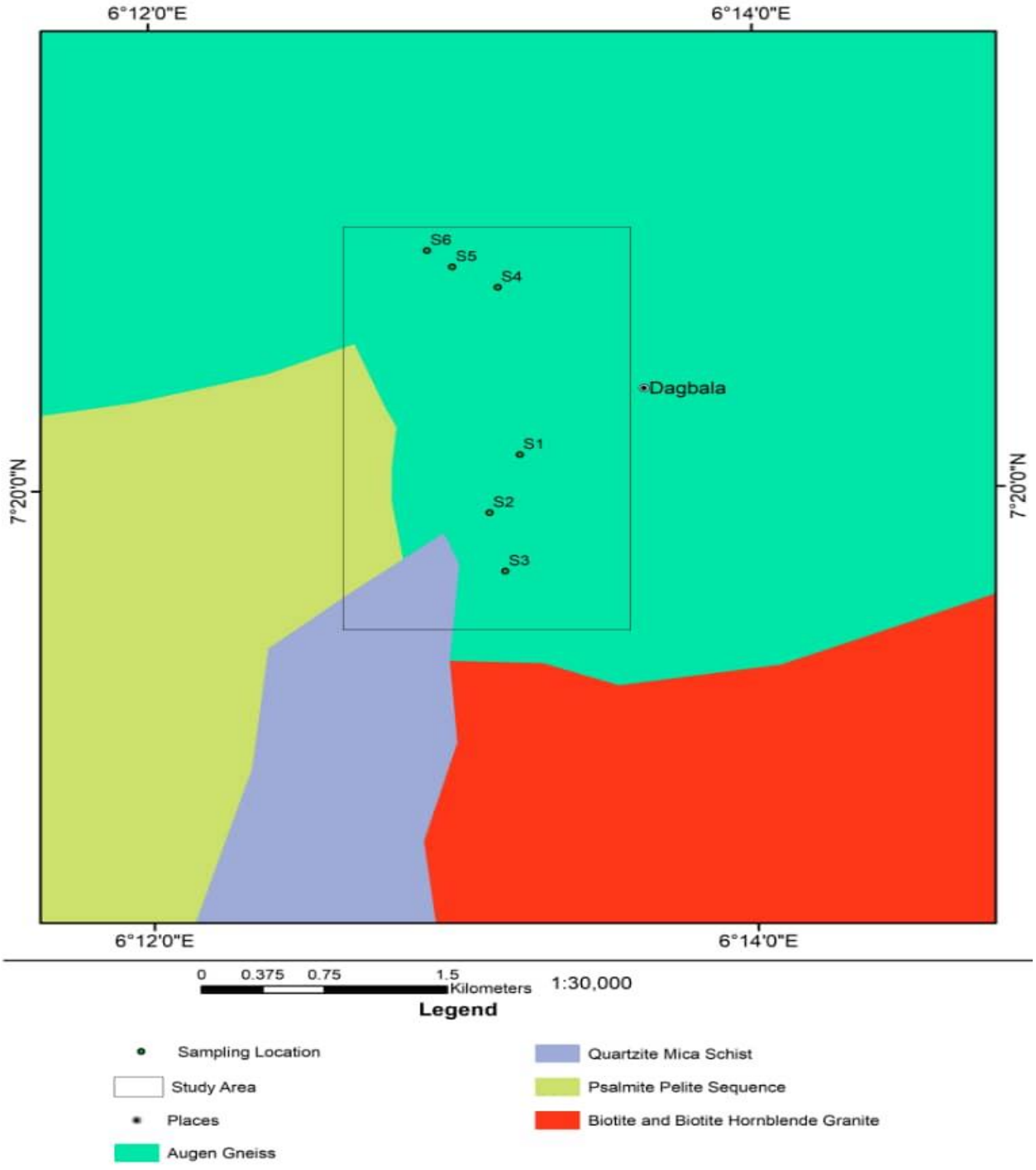

Fig 7: Geologic Map of Igarra Schist Belt indicating the area of study (adapted from NGSA , 2015).

CHAPTER THREE
MATERIALS AND METHODS

3.1 FIELD MAPPING

The mapping was done in two stages beginning with a reconnaissance survey for the purpose of familiarization with ground attributes of geologic features and to select access routes to reach outcrops identified from Google Earth map. A subsequent visit was carried between February 20th -23rd 2020 for detailed mapping.

Field mapping was carried out on a scale of 1:50,000 map. The field mapping was accomplished by selected transverses and use of field equipment such as Global positioning system (GPS), compass clinometer, sledge hammer, geologic hammer, field camera, cutlass, sample bag, field notebook, masking tape, pen etc.

3.2 MATERIALS USED

1. Global Positioning System (GPS): This is used to measure various coordinate readings of various locations encountered and the elevation above sea level of those areas.
2. Compass Clinometer: This is an instrument used to take the measurements of the strike and dip and dip direction of various plane surfaces. It is also used to tell the direction of movement from one point to another.
3. Geologic Hammer: This is a geologic instrument used to break outcrops that have noticeable plane of weakness.
4. Cutlass: This is used in the clearing of weeds in the field and for the digging of holes.
5. Field Camera: This is used to take snapshot of visual images on the field.
6. Sledge Hammer: This is used for cracking hard rocks on the field. They are also used as scale when taking pictures of outcrops and features on the outcrops.
7. Samples bag- This is used to store rock samples collected in the field which is further used for different analysis.
8. Field Notebook/Masking tape and pen- The field notebook is one of the most essential accessories used by a geologist in the field. This is due to the fact that records, details and

accurate measurement are documented with them for future references. Masking tape and pens are used for labeling samples before they are kept in the sample bag.

3.3 SAMPLE COLLECTION

In all, ten samples were collected out of which one was from an Augen-Gneiss host rock. Sampling interval for the rock samples varied depending on the aerial extent of each outcrop and field environmental conditions encountered. Samples 1 and 2 were obtained from location1, samples 3 and 4 from location 2, samples 5 and 6 from location 3, samples 7 and 8 from location 4, sample 9 was obtained from location 5 and sample 10 was obtained from location 6.

The samples were crushed and pulverized into fine powder at the Department of Geology, University of Benin. Thin sections of rock sample and polished sections of the Pegmatites were also made in the Department of Geology.

A total of ten samples were taken to Rolab Research and Diagnostic Laboratory at Ibadan, Oyo State, Nigeria for whole rock geochemical analysis using XRF technique to determine the major element composition present in the samples.

Plates 1-9 show pictures taken on the field during the mapping exercise.

Plate 1: Zonation of Pegmatite

Plate 2: Coarse Grain of Pegmatite Crystals

Plate 3: Contact between Pegmatite and Gneiss

Plate 4: Chilled Margin of Pegmatites

Plate 5: A Local Quarry of Pegmatites with Boulders

Plate 6: Charged Holes for Blasting

Plate 7: Sharp Contact between Pegmatite and Gneiss

Plate 8: Sharp Contact between Pegmatite and Gneiss

Plate 9: Overview of the Pegmatite Outcrop Visited at Dagballa

Plate 10: Samples from Different Locations Being Prepared for XRF and Thin Section Analysis

3.4 FIELD PRECAUTION

1. Only freshly broken samples were collected
2. Each sample was labeled according to the location obtained
3. Eye glasses were worn to when breaking samples from the rock body
4. Safety boots were worn for field protection.

3.5 METHODS

3.5.1 THIN SECTION ANALYSIS

A thin section (or petrographic thin section) is a thin slice of a rock, mineral etc. prepared in a laboratory for use with a polarizing petrographic microscope, electron microscope and electron microprobe. The sample has to be thin enough for light to pass through in a light microscope and have a polished surface for electron microscope studies.

STEPS INVOLVED IN THIN SECTION ANALYSIS

1. Cutting Slab: A suitable size slab for mounting on a slide is cut from a piece of rock with a cutter.
2. Initial Lapping of the Slab: The slab is labeled on one side and the other side is lapped flat and smooth first on a cast iron lap and then finished on a glass plate.
3. Glass Slide is Added: After drying on a hot plate, a glass slide is glued to the lapped face of the slab with epoxy.
4. Slab is Sectioned: Using a thin section saw, the slab is cut-off close to the slide. The thickness is further reduced on a thin section grinder.
5. Final Lapping: A finished thickness of 30 microns is achieved by lapping the section by hand on a glass plate with 600 grit carborundum. A fine grinding with 1000 grit prior to polishing is optional.
6. Polishing: The section is placed in a holder and spun on a polishing machine using nylon cloth and diamond paste until a suitable polish is achieved.

Plates 11-14 shows some of the equipment used during the thin section analysis.

Plate 11: A Rock Splitting Machine

Plate 12: A Gts1 Thin Section Cut-Off Saw

Plate 13: A Lapping/Polishing Machine

Plate 14: Petrographic Microscope

3.5.2 X-Ray Fluorescence (XRF) Machine

X-ray Fluorescence is an X-ray instrument used for relatively non-destructive chemical analyses of rocks, minerals, sediments and fluids. It works on wavelength dispersive spectroscopic principles that are similar to an electron microprobe (EPMA). But an XRF cannot make analysis at the small spot sizes typical of EPMA (2-5 microns). It is rather used for bulk analyses of large fractions of geological materials.

The XRF method depends on fundamental principles that are common to several other instrumental methods involving interactions between electron beams and X-ray with samples, including X-ray spectroscopy (e.g. SEM-EDS), X-ray diffraction (XRD) and wavelength dispersive spectroscopy (microprobe WDS). The analysis of major and trace elements in geological materials by X-ray fluorescence is made possible by the behavior of atoms when they interact with radiation with interaction. When materials are excited with high-energy, short wavelength radiation (e.g. X-rays), they can become ionized. If the energy of the radiation is sufficient to dislodge a tightly-held inner electron, the atom becomes unstable and an outer electron replaces the missing inner electron. When this happens, energy is released due to the decreased binding energy of the inner electron orbital compared with an outer one. The emitted radiation is of lower energy than the primary incident X-rays and is termed Fluorescent Radiation. Because the energy of the emitted photon is characteristic of a transition between specific electron orbitals in a particular element, the resulting fluorescent X-rays can be used to detect the abundances of elements that are present in the sample.

When the samples are illuminated by an intense X-ray beam known as the incident beam, some of the energy is scattered, but some is also absorbed within the sample in a manner that depends on its chemistry. The incident X-ray beam is typically produced from an Rh target. When this primary X-ray beam illuminates the sample, it is said to be excited. The excited sample in turn emits X-rays along a spectrum of wavelengths characteristic of the types of atoms present in the sample. The atoms in the sample absorb X-ray energy by ionizing, ejecting electrons from the lower (usually K and L) energy levels. The ejected electrons are replaced by electrons from an outer higher energy orbital. Energy is then released due to the decreased binding energy of the

inner electron orbital compared with an outer one. This energy released is in the form of emission of characteristic X-rays indicating the type of atom present.

CHAPTER FOUR

4.1 DISCUSSION AND INTERPRETATION OF RESULTS

The results obtained from thin section study conducted are presented in plates 15-24. The main components of the rock samples are quartz, feldspar (microcline and albite), mica and some opaque minerals. This class of mineral assemblage indicates emplacement in continental environment (Ayodele, 2015). From the analysis, quartz and microcline represents the dominant mineral components of the rocks.

Quartz is present in all the rock samples with a percentage range of 10-40%. The quartz crystals are colorless and clear, lacking any form of cleavages. They show first other polarization colors of grey to white (Dyar and Gunter, 2008). Some of the quartz crystals show straight extinction while fractured and dislocated ones show undulose extinction (McNamee and Gunter, 2014).

Microcline is the major feldspar mineral present in the samples with compositions ranging between 30-80%; they likely indicate granite origin (Imasuen *et al*, 2013). It is colorless and cloudy, showing alterations to sericite. It is recognized by its characteristic grid (cross-hatched) twinning under crossed-polarized light (McNamee and Gunter, 2014). It also occurs as anhedral-subhedral crystals with low relief and it exhibits no pleochroism (Dyar and Gunter, 2008).

The biotite mica is strongly pleochroic in shades of brown to dark brown, it has a good cleavage, which is anhedral to subhedral with moderate under plane polarized light (Dyar and Gunter, 2008). It displays a near parallel extinction and exhibits a high birefringence under cross polarized light (Dyar and Gunter, 2008). It occurs in traces and occupies between 5-30% of the entire mineral composition of the rock samples.

The results from the XRF analysis of the samples are summarized in tables 6 and 7. The results were used to create bivariate plots with regression analysis, bar charts, compute alumina saturation index of samples and correlation coefficients

4.2 PHOTOMICROGRAPHS FROM PETROGRAPHIC MICROSCOPE

Photomicrographs from petrographic microscope shows that the dominant minerals present in most of the samples are quartz, feldspar minerals which include microcline, albite and orthoclase, mica minerals such as muscovite and biotite. The following characteristics of minerals under the microscope were used to distinguish the various minerals, they include:

4.2.1 Relief: The speed of light slows down when it enters a material from air. This change is described by the material's refractive index. Relief describes the difference of refractive index of the mineral of interest to the surrounding material (McNamee and Gunter, 2014). Albite, quartz and microcline display low relief.

4.2.2 Transparent or Opaque Minerals: Transparent minerals are minerals that allows light to pass through them under plane polarized microscopy while opaque minerals are minerals that absorb light under the microscope. Quartz and felsic minerals are examples of transparent minerals under the petrographic microscope while hornblende is an example of an opaque mineral under the microscope (Dyar and Gunter, 2008).

4.2.3 Pleochroism: This is when a mineral changes color as it is rotated relative to the polarizer in plane polarized light. Felsic minerals do not exhibit pleochroism under plane polarized light (Dyar and Gunter, 2008).

4.2.4 Cleavage: This is the tendency of a mineral to break along a plane of weakness (McNamee and Gunter, 2014). Muscovite exhibits one direction cleavage, quartz shows no cleavage while microcline exhibits cleavage in one and two directions.

4.2.5 Twinning: In crystallography, this is the regular intergrowth of two or more crystal grains so that each grain is a reflected image of is neighbor or is rotated with respect to it. Albite exhibits carlsbad twinning while microcline exhibits cross-hatch twinning.

4.3 BIVARIATE PLOT WITH REGRESSION ANALYSIS

The correlation coefficient (r) represents the relationship between the independent variable (SiO_2) and the dependent variables (other major oxides). A positive correlation coefficient indicates that as the value of the independent variable increases, the mean of the dependent variable also tends to increase.

The association of silica (SiO_2) with phosphate (P_2O_5) shows a significant positive correlation with a correlation coefficient of 0.1720, but when plotted alongside with the values obtained from Lokoja and Lema-Ndeji, there is a significant negative correlation and the correlation coefficient becomes 0.2362.

The association of silica (SiO_2) with titanium oxide (TiO_2) shows a significant negative correlation with a correlation coefficient of 0.8786 and the negative correlation is also observed when plotted alongside with the values obtained from Lokoja and Lema-Ndeji and the correlation coefficient becomes 0.7498.

The association of silica (SiO_2) with soda (Na_2O) shows a significant positive correlation with a correlation coefficient of 0.6089 and the positive correlation is also observed when plotted alongside with the values obtained from Lokoja and Lema-Ndeji and the correlation coefficient becomes 0.6581.

The association of silica (SiO_2) with potash (K_2O) shows a significant negative correlation with a correlation coefficient of 0.3183, but when plotted alongside with the values obtained from

Lokoja and Lema-Ndeji, there is a significant positive correlation and the correlation coefficient becomes 0.7622.

The association of silica (SiO_2) with iron oxide (Fe_2O_3) shows a significant negative correlation with a correlation coefficient of 0.8700 and the negative correlation is also observed when plotted alongside with the values obtained from Lokoja and Lema-Ndeji and the correlation coefficient becomes 0.8476.

The association of silica (SiO_2) with phosphate (Al_2O_3) shows a significant positive correlation with a correlation coefficient of 0.8086, but when plotted alongside with the values obtained from Lokoja and Lema-Ndeji, there is a significant negative correlation and the correlation coefficient becomes 0.01.

The association of silica (SiO_2) with iron oxide (MgO) shows a significant negative correlation with a correlation coefficient of 0.4709 and the negative correlation is also observed when plotted alongside with the values obtained from Lokoja and Lema-Ndeji and the correlation coefficient becomes 0.5098.

The association of silica (SiO_2) with iron oxide (CaO) shows a significant negative correlation with a correlation coefficient of 0.7849 and the negative correlation is also observed when plotted alongside with the values obtained from Lokoja and Lema-Ndeji and the correlation coefficient becomes 0.7622.

The association of silica (SiO_2) with iron oxide (MnO) shows a significant negative correlation with a correlation coefficient of 0.5611 and the negative correlation is also observed when plotted alongside with the values obtained from Lokoja and Lema-Ndeji and the correlation coefficient becomes 0.6166.

The correlation coefficient obtained for the various plots are shown in figure 8 to figure 25.

4.4 MAJOR OXIDES IN ALL THE SAMPLES

Al_2O_3 abundances range from 14.57% to 15.61% with DA8 which was obtained from the host rock having the lowest value and DA7 having the highest value. The range of values of alumina across all the rock samples analyzed, is relatively uniform. These values are quite less than the mean values of 16.98% (Omoruyi, 2021) and 16.05% (Okunlola, 2008) obtained from analysis of Pegmatite samples in Lokoja and Lema-Ndeji, respectively.

CaO abundances for all the samples is fairly uniform (<1%), and it is identical to the mean values obtained from analysis of Pegmatites in Lokoja and Lema-Ndeji with the exception being DA8 (2.30%) which was obtained from the host rock.

Na_2O abundances range from 2.76% to 5.56% with DA1 having the lowest value while DA3, DA6, and DA9 have the highest values. The host rock contains a slightly lesser value (2.88%) compared to other samples obtained. The mean value obtained from Lokoja (4.334%) falls within the range obtained but that of Lema-Ndeji (1.78%) is quite less than the values obtained.

K_2O abundances range from 3.50% to 8.43%. DA1, DA2, DA3, DA5, DA6, DA9 and DA10 occur in similar range of values (8.05—8.43%), while DA4 and DA7 have similar range of 3.50% and 3.52% respectively. The mean value obtained from Lokoja (6.672%) falls within the range obtained but that of Lema-Ndeji (1.41%) is quite less than the values obtained.

MgO abundances are relatively low (0.05-0.14%). Fe_2O_3 values are also low ranging from 0.30-0.47% except for sample 8 (5.82%) which is from the host rock and it is close to the mean value obtained from Lema-Ndeji (4.59%). The mean value obtained from Lokoja for Fe_2O_3 is 0.74%.

4.5 ALUMINA SATURATION INDEX

The Alumina Saturation Index which is defined by molecular ratio $Al_2O_3/(CaO+Na_2O+K_2O)$ {A/CNK} is used to classify rocks into metaluminous (A/CNK<1); peraluminous (A/CNK>1); or peralkaline (A<NK) {Frost and Frost, 2008}. The computation of A/CNK for the pegmatites showed that the rock samples analyzed were all peraluminous and therefore implied a relationship to S-type granites (*Cerny et al. 2012*). Peraluminous granites are generally considered to be generated through partial melting of upper crustal rocks; especially during continent-continent collision events (*Turpin et al. 1990*). The following values were obtained:

- DA1; 1.657 (peraluminous)
- DA2; 1.564 (peraluminous)
- DA3; 1.154 (peraluminous)
- DA4; 1.686 (peraluminous)
- DA5; 1.560 (peraluminous)
- DA6; 1.164 (peraluminous)
- DA7; 1.738 (peraluminous)
- DA8; 1.360 (peraluminous)
- DA9; 1.160 (peraluminous)
- DA10; 1.416 (peraluminous)

These values show that all the pegmatite samples are peraluminous with DA7 and DA9 being the most peraluminous and least peraluminous respectively.

4.6 TEST OF SIGNIFICANCE OF OBSERVED CORRELATION COEFFICIENTS

The significance of the observed correlation coefficient results presented is shown in Table 9. Out of the 45 correlations found between two parameters (major oxides), 13 were found to have significance at 1% ($P<0.01$) level. A very strong positive correlation exist between SiO_2 and Al_2O_3 (0.809), TiO_2 and Fe_2O_3 (1.000), TiO_2 and MgO (0.767), TiO_2 and CaO (0.924), Fe_2O_3 and MgO (0.773), Fe_2O_3 and CaO (0.926), MnO and MgO (0.861). The high degree of positive correlations between the pair of oxides probably indicates a similar source in the formation of the oxides in the samples. The negative correlations were found between SiO_2 and TiO_2 (-0.879), SiO_2 and Fe_2O_3 (-0.870), SiO_2 and CaO (-0.785), TiO_2 and Al_2O_3 (-0.755), MnO and P_2O_5 (-0.827), MgO and P_2O_5 (-0.824).

4.7 DENDROGRAM SHOWING THE RELATIONSHIP BETWEEN MAJOR OXIDES

A dendrogram is a branching diagram that represents the relationships of similarity among a group of entities. These entities are usually divided into clusters in the dendrogram with the components in each cluster showing similar characteristics in terms of origin or source.

The dendrogram gotten from the analysis divides the major oxides into four clusters. The clusters gotten from the dendrogram, indicates the following:

- Cluster 1: MgO, K_2O and Al_2O_3.
- Cluster 2: MnO, P_2O_5, TiO_2 and SiO_2.
- Cluster 3: Fe_2O_3 and CaO.
- Cluster 4: Na_2O

The oxides present in each of the individual clusters obtained, shows the oxides probably have similar origin to each other i.e. they are obtained from the same source. From the dendrogram obtained, Na_2O shows a distant relationship with the other clusters present indicating it has a similar origin to the other oxides present in all the samples collected.

4.8 TRACE ELEMENT COMPOSITION

Average values for the chemical data for the trace elements are presented in Table 10. The elements present in substantial amounts include Barium (Ba), Cesium (Ce), Rubidium (Rb), Tantalum (Ta), Strontium (Sr), Niobium (Nb). The results show the pegmatites are enriched in rare metals with moderately high values of Ba (14040ppm), Ta (730ppm), Cs (450ppm), Rb (408ppm). Also from the average values of 730ppm for Ta and 58ppm for Nb, the pegmatite bodies are not comparable with moderately endowed Ta-Nb pegmatites globally (Cerny, 1989).

The Rb/Sr ratio (2.81) is fairly comparable with most of the other rare metal pegmatites of Nigeria. Similarly, average K/Rb value (0.01) is comparable with the average for the rare metal pegmatite of Nigeria (Okunlola, 2005). These values may indicate probable mineralization and progressive fractionation (Kuster, 1990).

Table 6: Major Oxide Compositions from Sampling Points and Lokoja and Lema-Ndeji

Major Element (%)	SP1	SP2	SP3	SP4	SP5	SP6	SP7	SP8	SP9	SP10	A	B
SiO2	72.03	72.02	72.70	74.95	72.06	72.51	74.47	66.75	72.51	72.03	70.58	69.38
TiO2	0.01	0.01	0.02	0.01	0.01	0.02	0.01	0.55	0.02	0.01	0.042	0.802
Al2O3	15.20	15.09	15.15	15.13	15.05	15.36	15.61	14.57	15.36	15.05	16.98	16.05
Fe2O3	0.36	0.30	0.47	0.40	0.31	0.45	0.40	5.82	0.45	0.31	0.74	4.59
MnO	0.06	0.02	0.02	0.04	0.02	0.02	0.04	0.08	0.02	0.02	0.032	0.08
MgO	0.10	0.10	0.05	0.14	0.07	0.06	0.12	0.20	0.06	0.07	0.108	0.41
CaO	0.09	0.12	0.70	0.27	0.09	0.72	0.27	2.30	0.75	0.09	0.898	0.72
Na2O	2.76	3.35	5.56	5.28	3.37	5.55	5.28	2.88	5.56	3.40	4.334	1.78
K2O	8.43	8.05	8.20	3.50	8.08	8.20	3.52	6.15	8.20	8.05	6.672	1.41
P2O5	0.30	0.45	0.40	0.22	0.45	0.40	0.22	0.16	0.36	0.48	0.019	1.54

SP (Sampling Points); Dangballa , A: Lokoja, Central Nigeria [n=5] (Omoruyi and Imeokparia 2021), B: Lema-Ndeji, Central Nigeria [n=20] (Okunlola and Akintola 2008)

Table 7: Summary of Major Oxides with Statistical Parameters

Major Element (%)	SP1	SP2	SP3	SP4	SP5	SP6	SP7	SP8	SP9	SP10	Min	Max	Mean	Std. Dev.	Var.
SiO2	72.03	72.02	72.7	74.95	72.06	72.51	74.47	66.75	72.51	72.03	66.75	74.95	72.20	2.18	4.77
TiO2	0.01	0.01	0.02	0.01	0.01	0.02	0.01	0.55	0.02	0.01	0.01	0.55	0.067	0.17	0.029
Al2O3	15.2	15.09	15.15	15.13	15.05	15.36	15.61	14.57	15.36	15.05	14.57	15.61	15.16	0.27	0.073
Fe2O3	0.36	0.3	0.47	0.4	0.31	0.45	0.4	5.82	0.45	0.31	0.3	5.82	0.93	1.72	2.96
MnO	0.06	0.02	0.02	0.04	0.02	0.02	0.04	0.08	0.02	0.02	0.02	0.08	0.034	0.021	0.00044
MgO	0.1	0.1	0.05	0.14	0.07	0.06	0.12	0.2	0.06	0.07	0.05	0.2	0.097	0.046	0.0021
CaO	0.09	0.12	0.7	0.27	0.09	0.72	0.27	2.3	0.75	0.09	0.09	2.3	0.54	0.68	0.46
Na2O	2.76	3.35	5.56	5.28	3.37	5.55	5.28	2.88	5.56	3.4	2.76	5.56	4.30	1.23	1.51
K2O	8.43	8.05	8.2	3.5	8.08	8.2	3.52	6.15	8.2	8.05	3.5	8.43	7.04	1.97	3.87
P2O5	0.3	0.45	0.4	0.22	0.45	0.4	0.22	0.16	0.36	0.48	0.16	0.48	0.34	0.11	0.013

PHOTOMICROGRAPHS OF VARIOUS SAMPLES

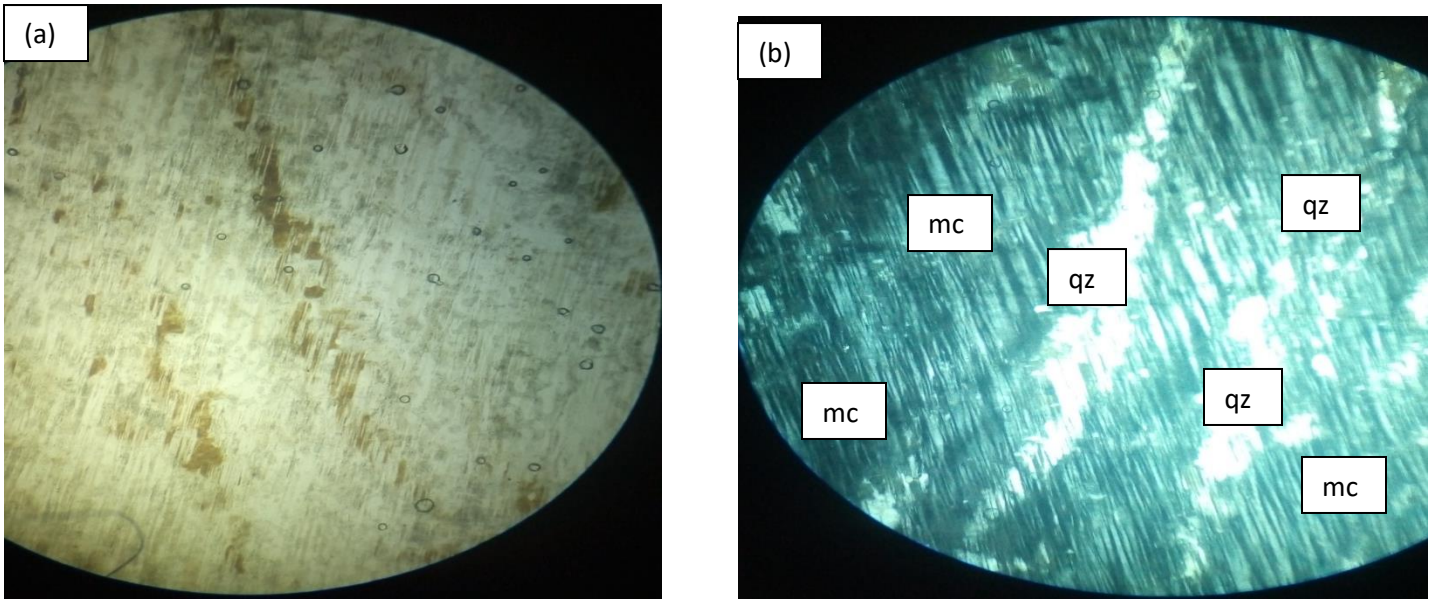

Plate 15: Photomicrograph of Sample 1 pegmatite (a) under PPL and (b) under XPL x40; op-opaque, qz-quartz, mc-microline

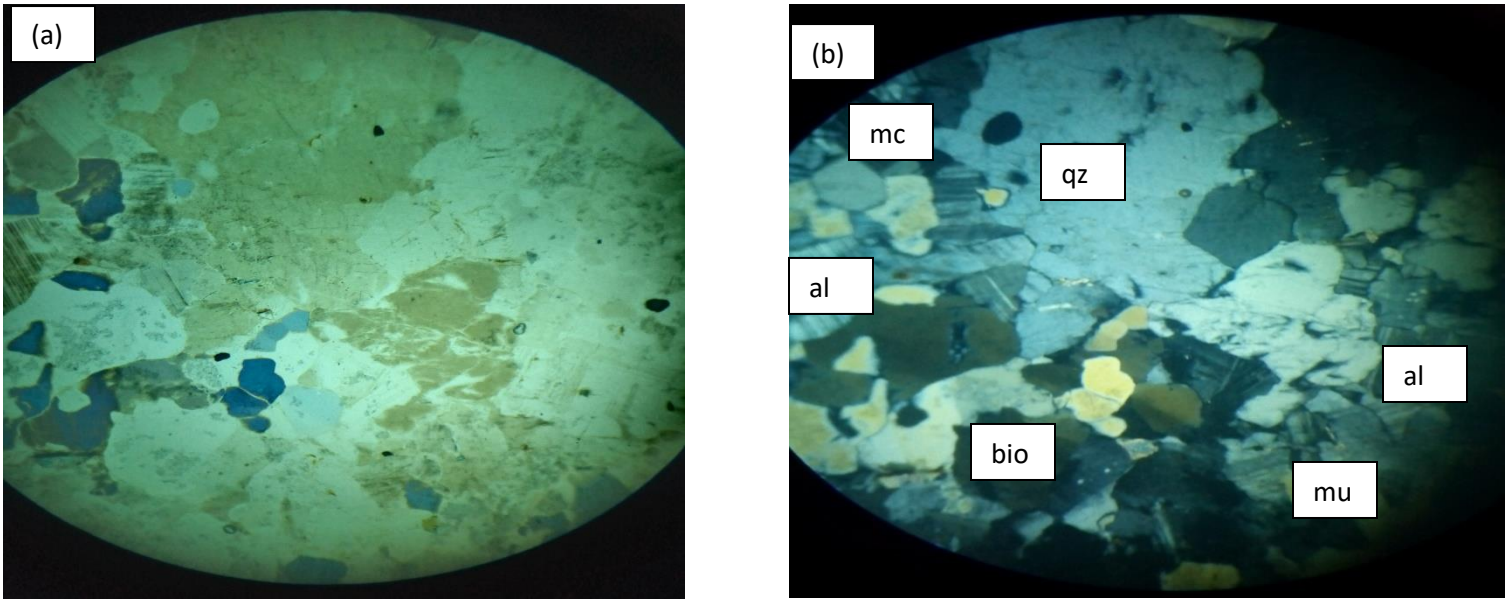

Plate 16: Photomicrograph of Sample 2 pegmatite (a) under PPL and (b) under XPL x40; op-opaque, qz-quartz, mc-microline, bio-biotite, mus-muscovite, al-albite

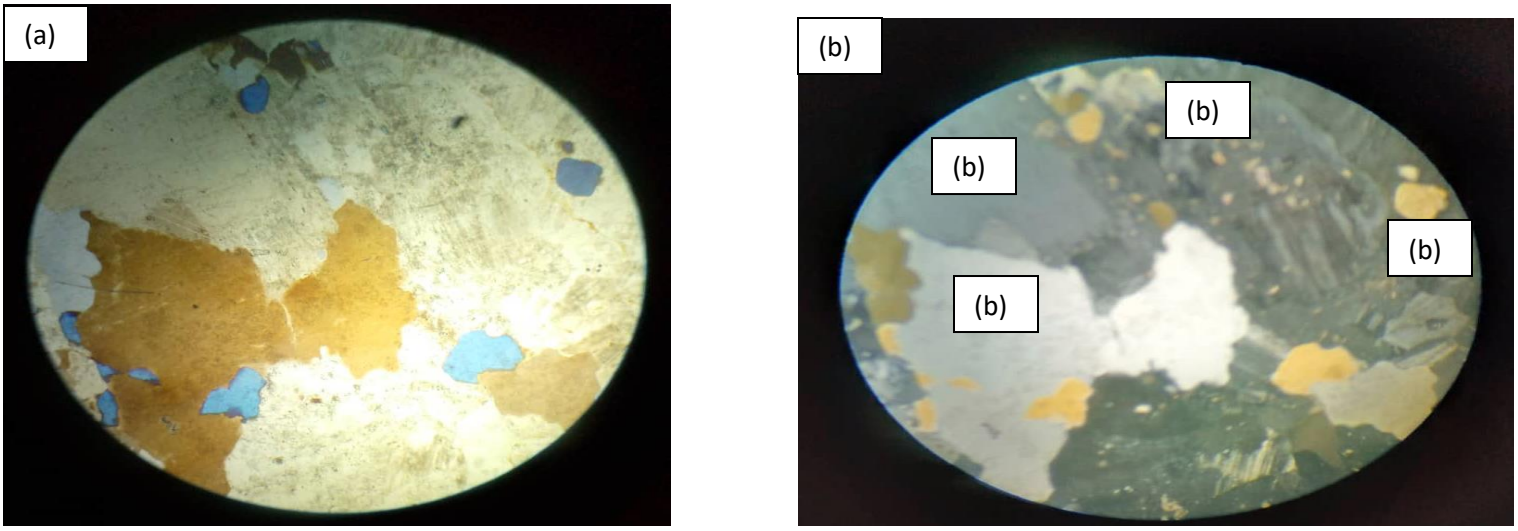

Plate 17: Photomicrograph of Sample 3 pegmatite (a) under PPL and (b) under XPL x40; op-opaque, qz-quartz, mc-microline, bio-biotite, mus-muscovite.

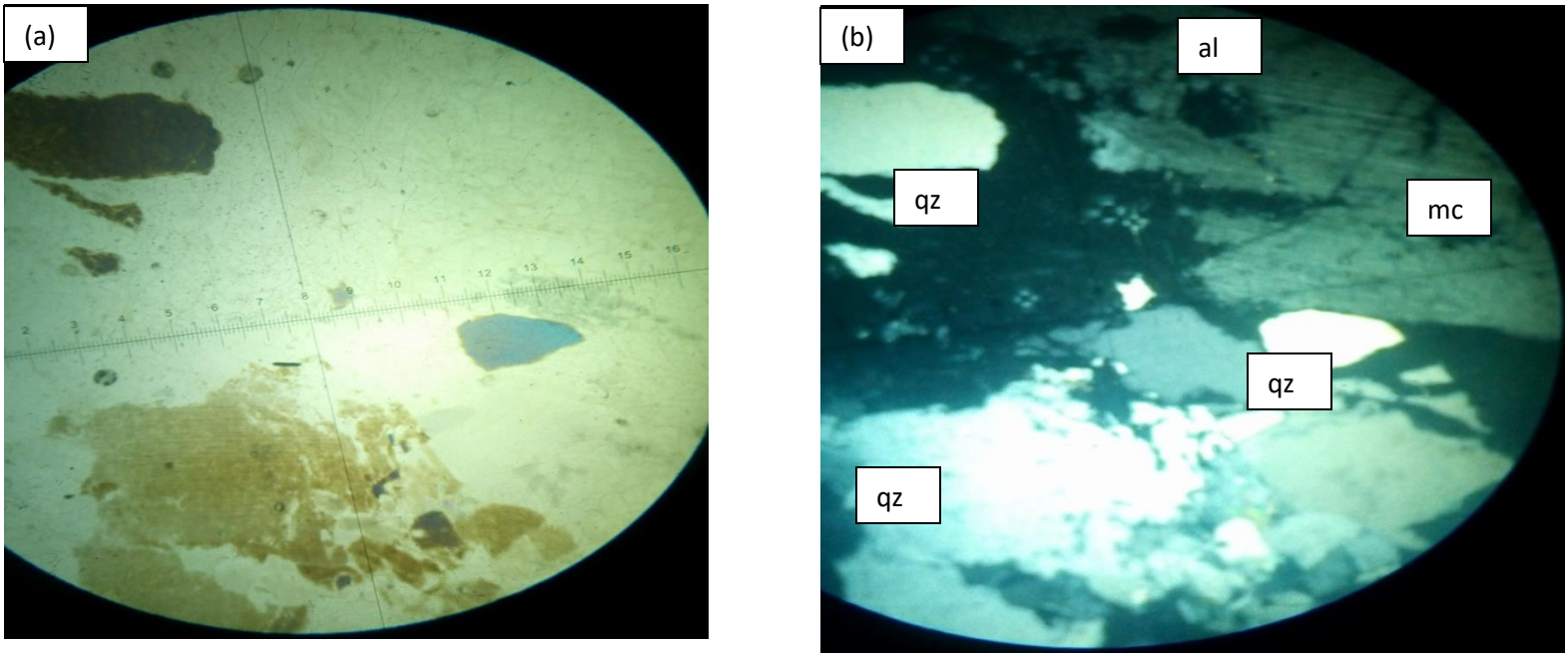

Plate 18: Photomicrograph of Sample 4 pegmatite (a) under PPL and (b) under XPL x40; op-opaque, qz-quartz, mc-microline, bio-biotite, mus-muscovite, al-albite

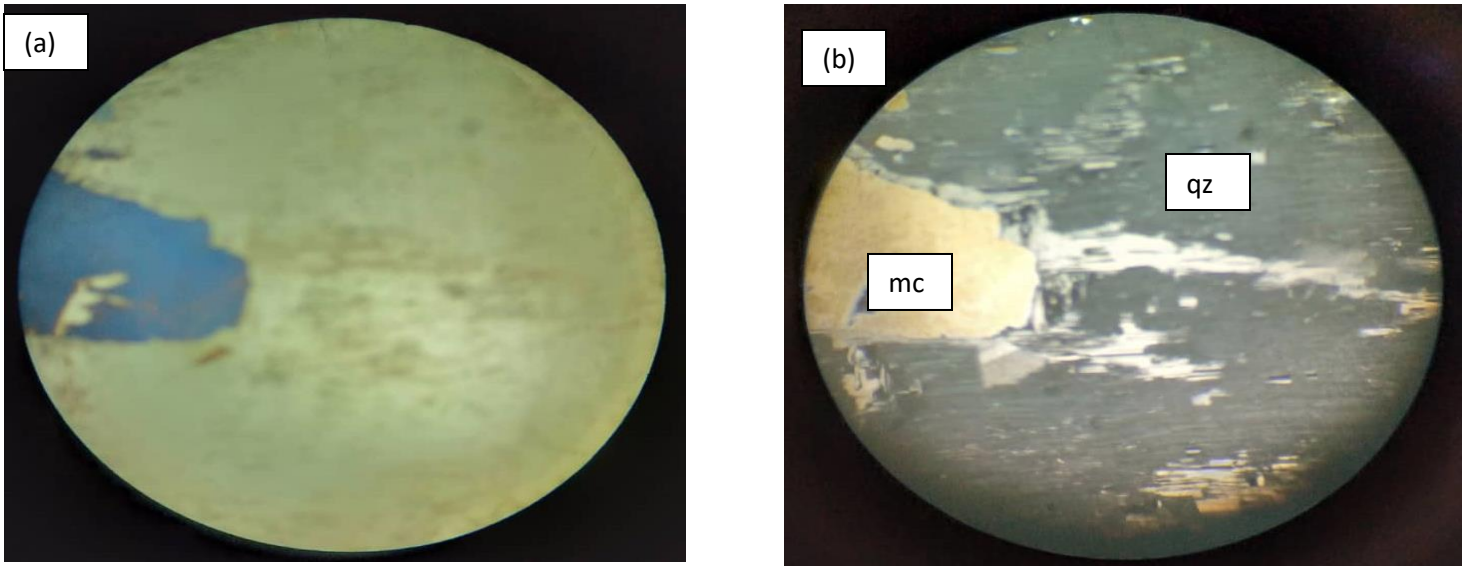

Plate 19: Photomicrograph of Sample 5 pegmatite (a) under PPL and (b) under XPL x40; op-opaque, qz-quartz, mc-microline

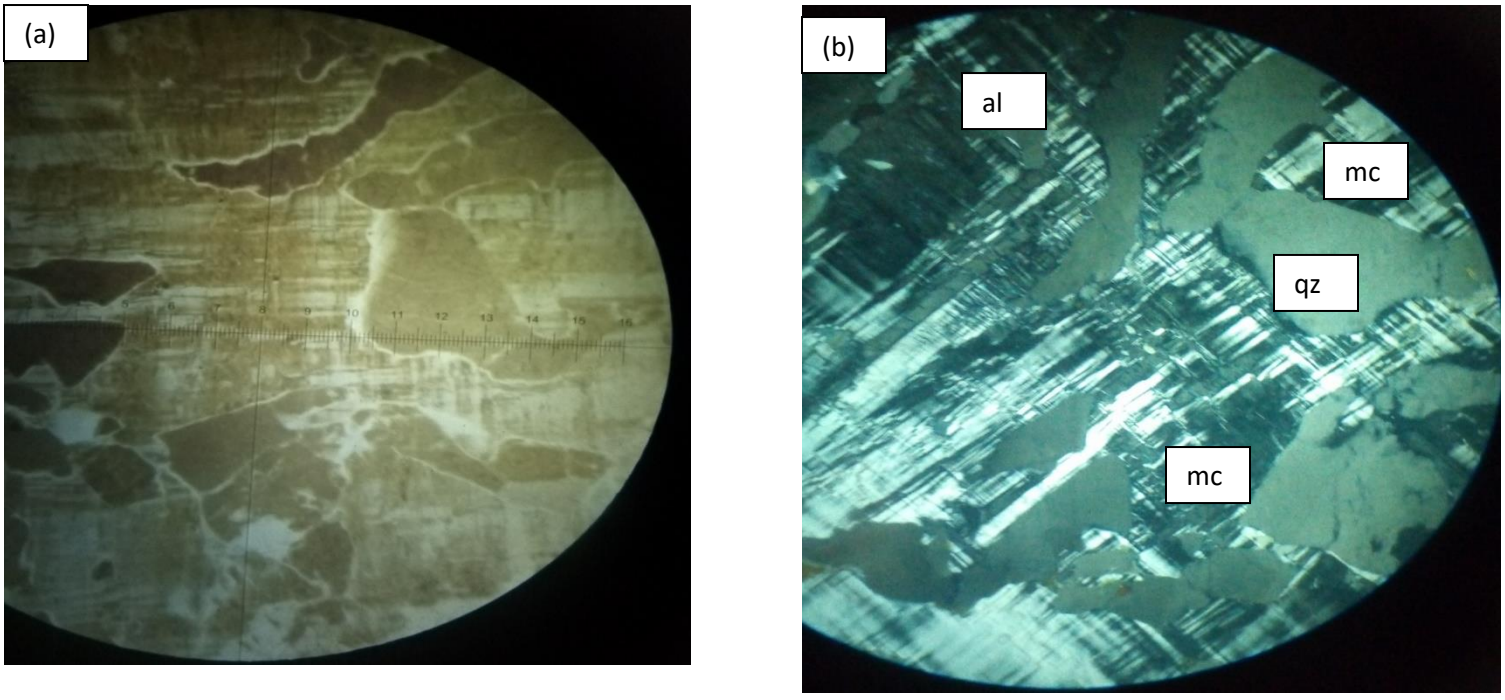

Plate 20: Photomicrograph of Sample 6 pegmatite (a) under PPL and (b) under XPL x40; op-opaque, qz-quartz, mc-microline, al-albite

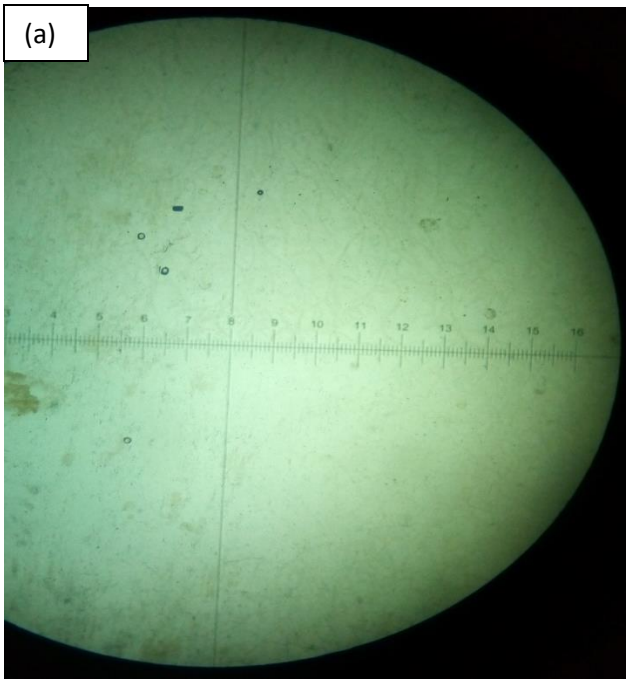

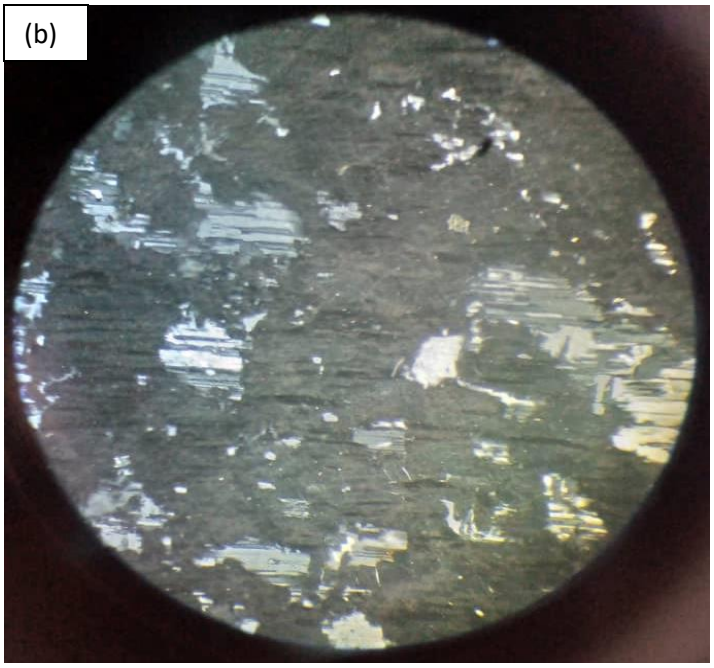

Plate 21: Photomicrograph of Sample 7 pegmatite (a) under PPL and (b) under XPL x40; op-opaque, qz-quartz, mc-microline

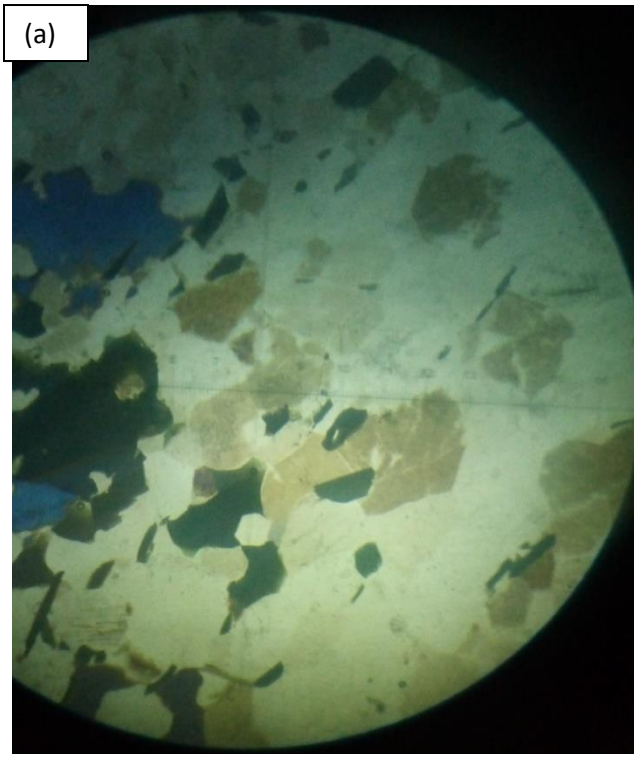

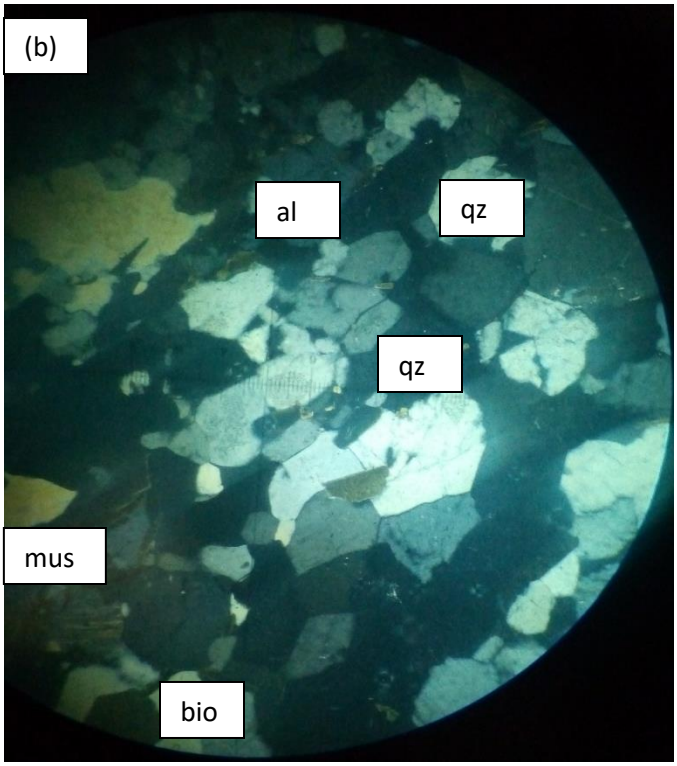

Plate 22: Photomicrograph of Sample 8 Augen-Gneiss (a) under PPL and (b) under XPL x40; op-opaque, qz-quartz, mc-microline, bio-biotite, mus-muscovite, al-albite

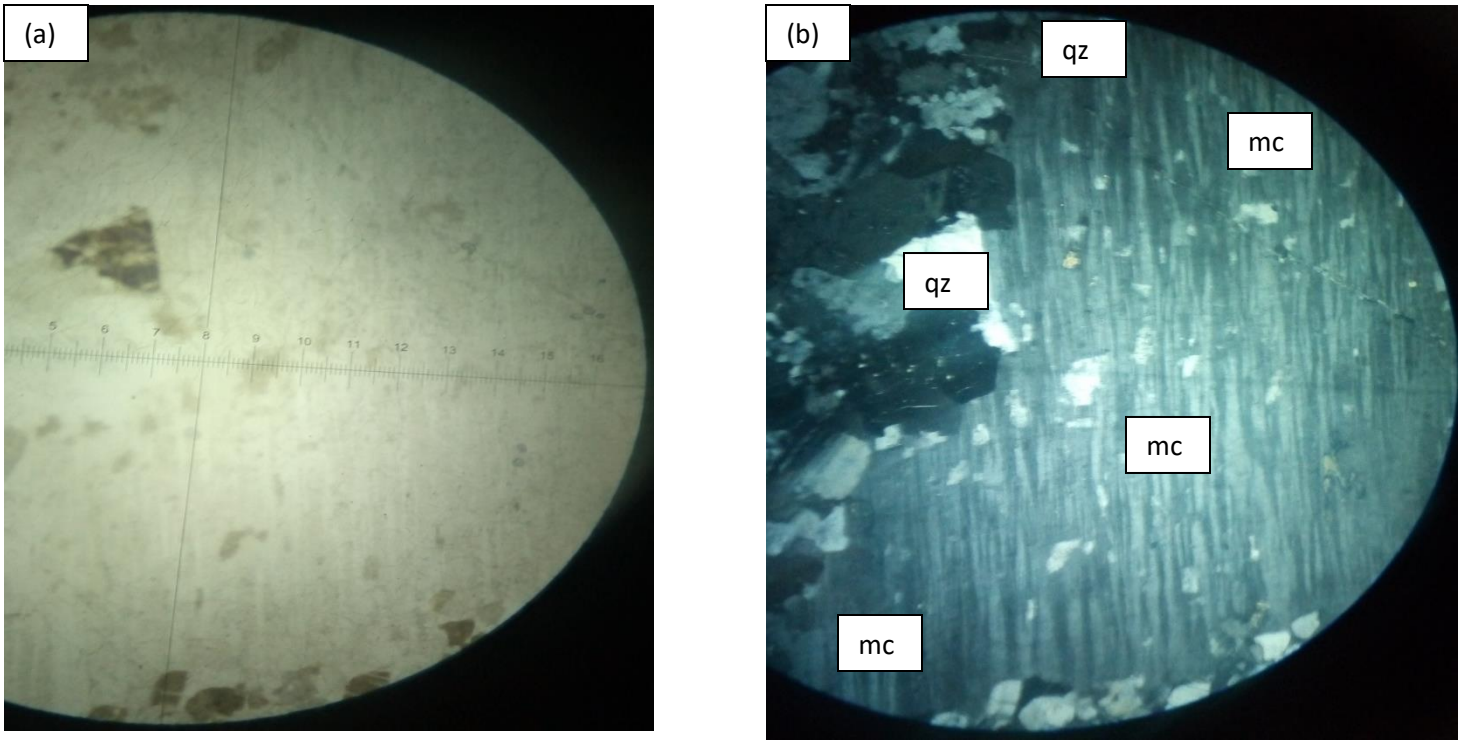

Plate 23: Photomicrograph of Sample 9 pegmatite (a) under PPL and (b) under XPL x40; op-opaque, qz-quartz, mc-microline

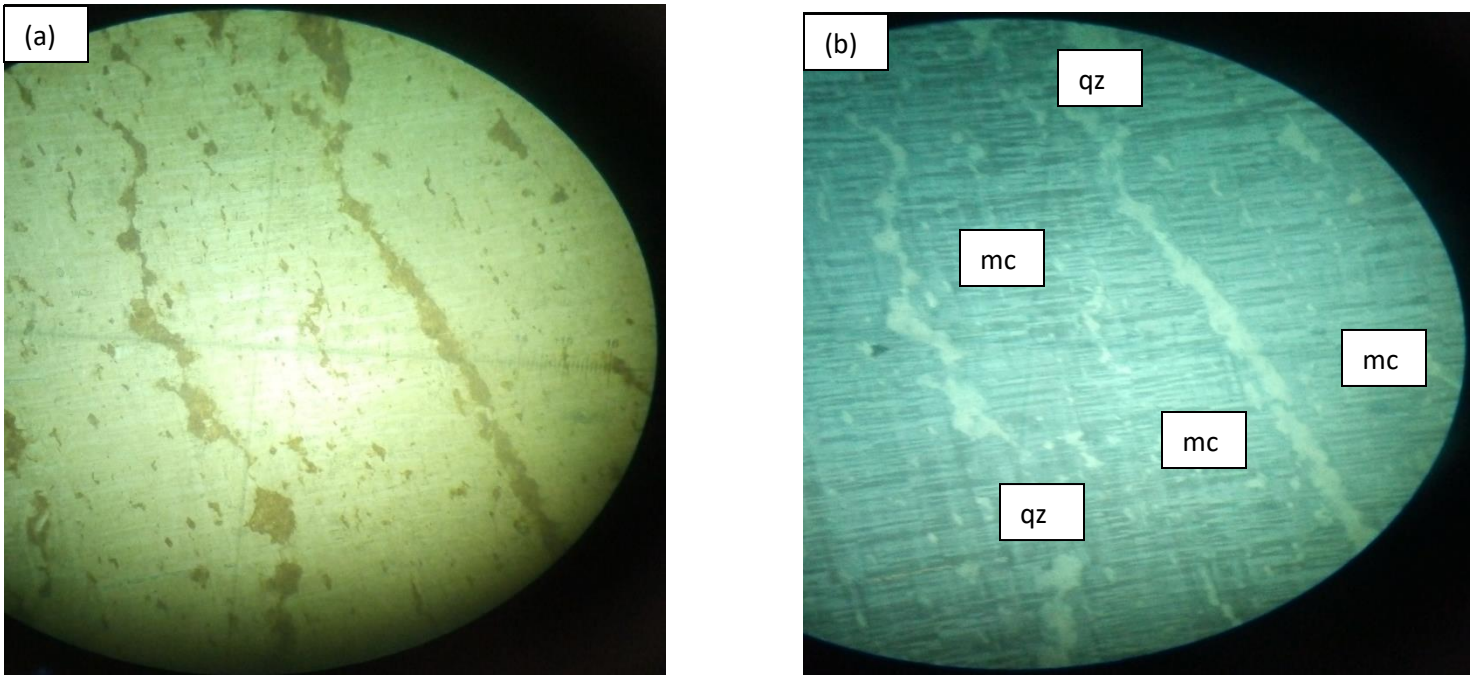

Plate 24: Photomicrograph of Sample 10 pegmatite (a) under PPL and (b) under XPL x40; op-opaque, qz-quartz, mc-microline

Table 8: Average Modal Composition of Samples

Mineral	Visual Estimation %
DA1	
Quartz	20
Microcline	70
Opaque	10
DA2	
Quartz	25
Microcline	30
Biotite	15
Muscovite	15
Opaque	5
Albite	10
DA3	
Microcline	50
Quartz	40
Biotite	5
Muscovite	5
DA4	
Microcline	50
Quartz	30
Biotite	6
Opaque	4
Albite	10
DA5	
Microcline	80
Quartz	20
DA6	
Microcline	50
Quartz	40
Albite	10
DA7	
Microcline	75
Quartz	25
DA8	
Opaque	5
Quartz	30
Microcline	35
Biotite	10
Muscovite	10
Albite	10
DA9	
Microcline	90
Quartz	10
DA10	
Microline	85
Quartz	15

BIVARIATE PLOTS OF DIFFERENT OXIDES AGAINST SiO_2

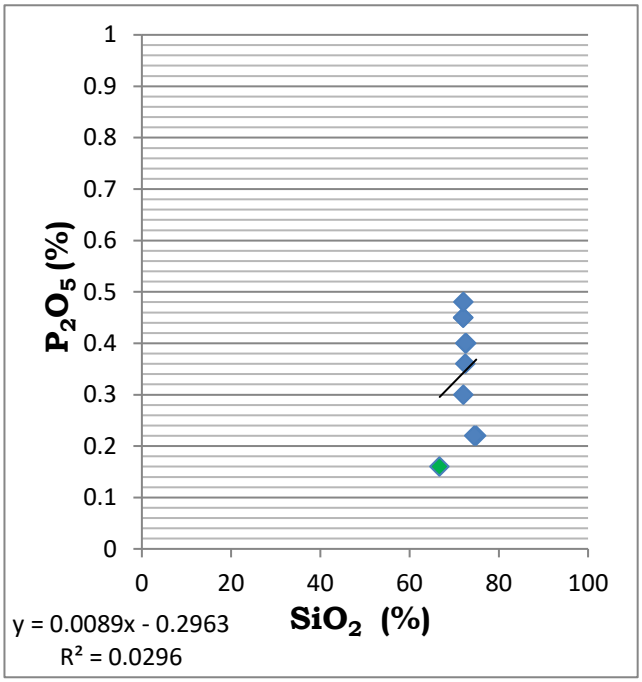

Fig 8: P_2O_5 Against SiO_2

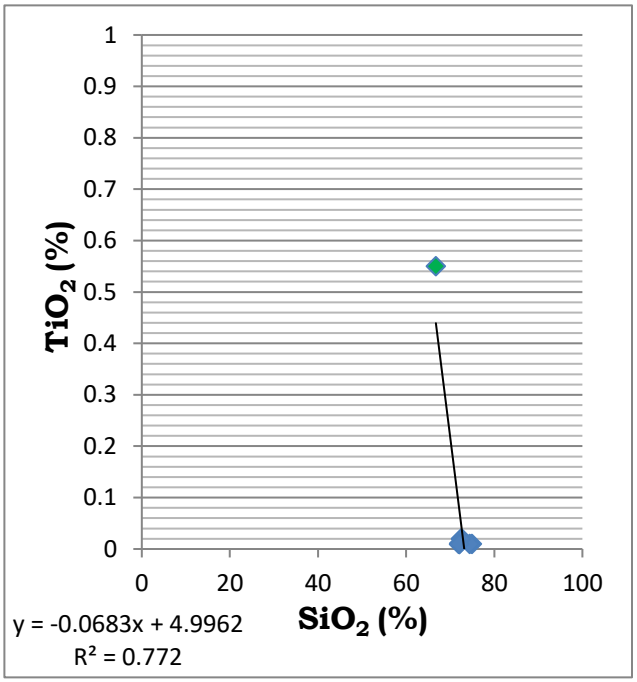

Fig 9 TiO_2 Against SiO_2

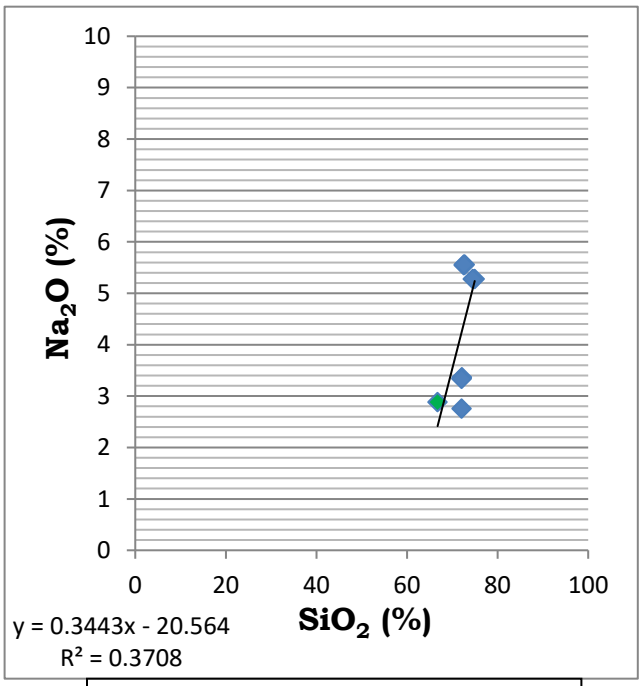

Fig 10: Na_2O Against SiO_2

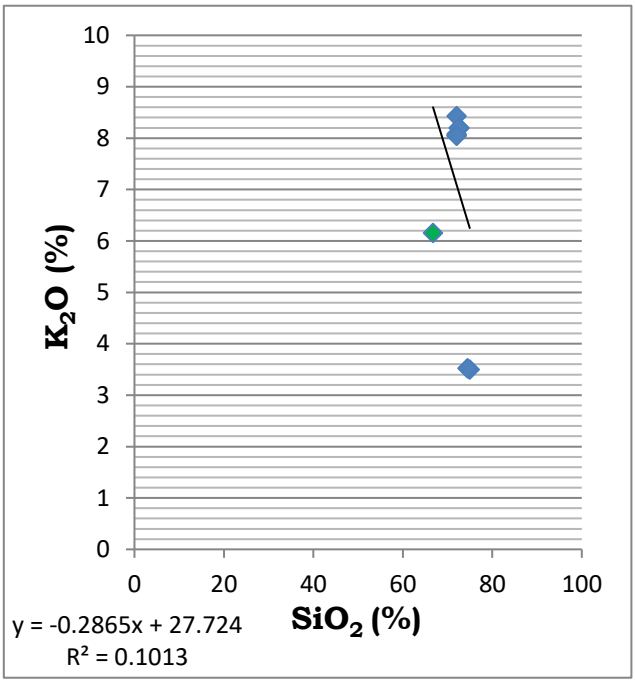

Fig 11: K_2O Against SiO_2

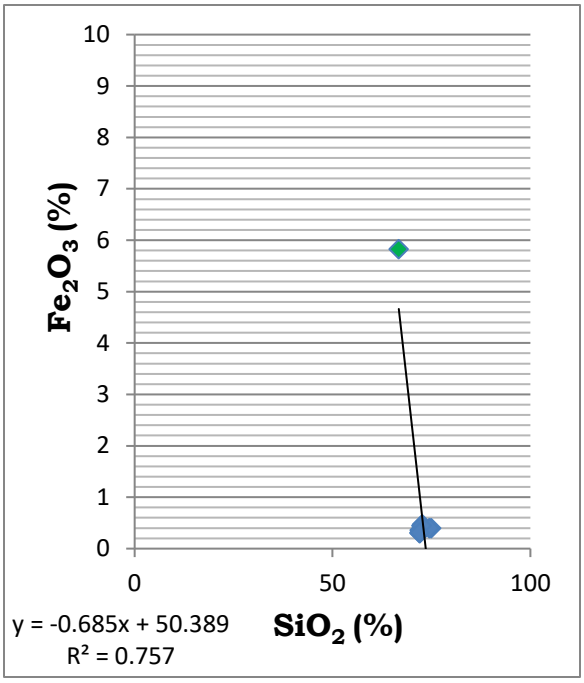

Fig 12: SiO_2 Against Fe_2O_3

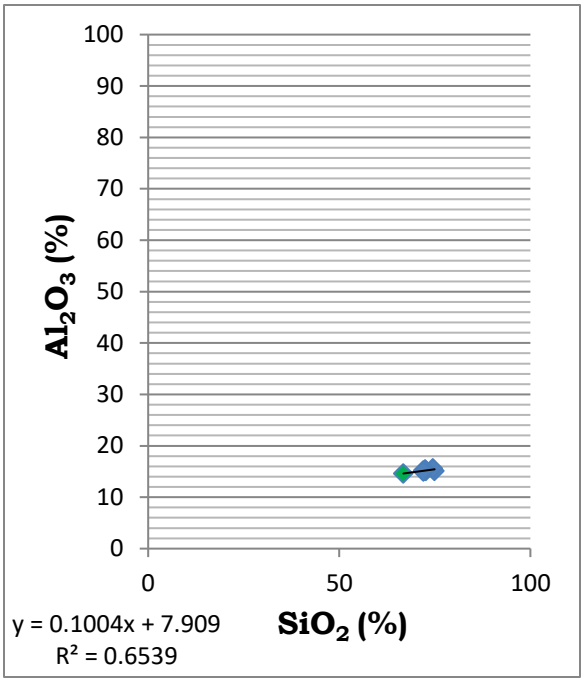

Fig 13: SiO_2 Against Al_2O_3

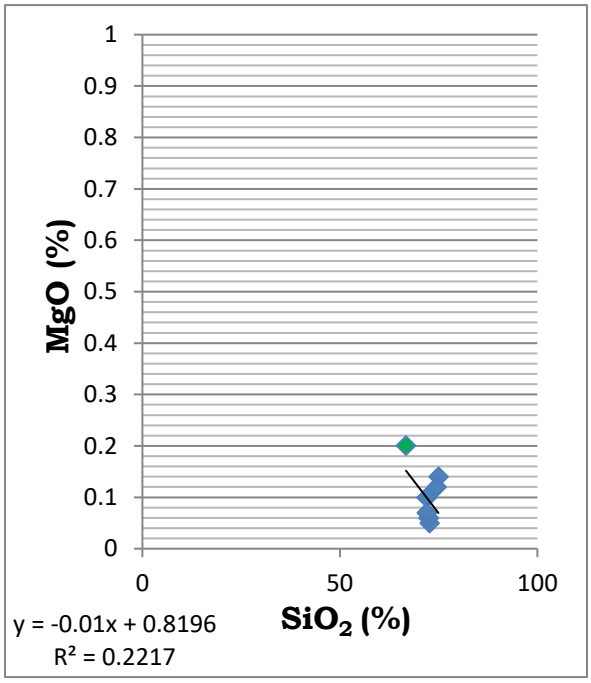

Fig 14: SiO_2 Against MgO

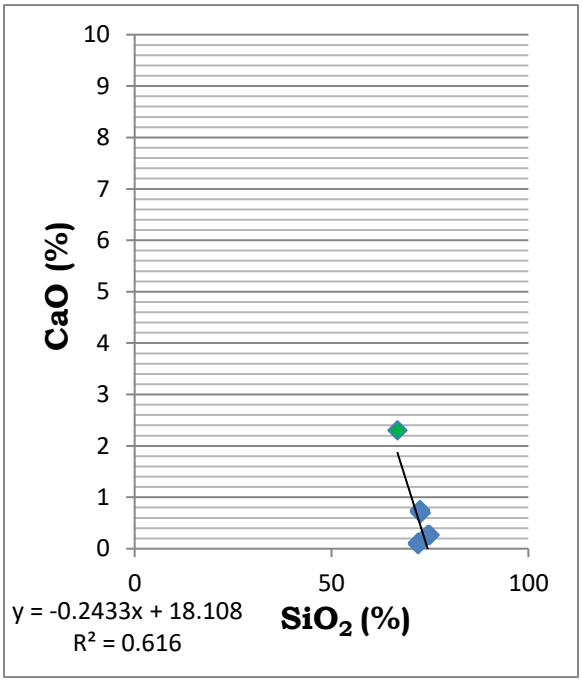

Fig 15: SiO_2 Against CaO

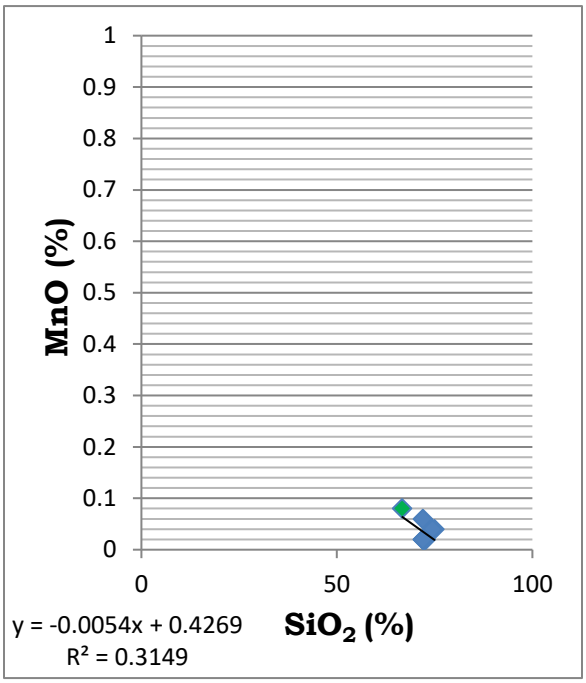

Fig 16: SiO_2 Against MnO

Legend for Bivariate Plots

LOCATION	COLOUR MARKER
DANGBALLA	BLUE
HOST ROCK DANGBALLA	GREEN

BIVARIATE PLOTS OF OXIDES AGAINST SIO_2 COMPARED TO OMORUYI AND IMEOKPARIA (2021), OKUNLOLA AND AKINTOLA (2008)

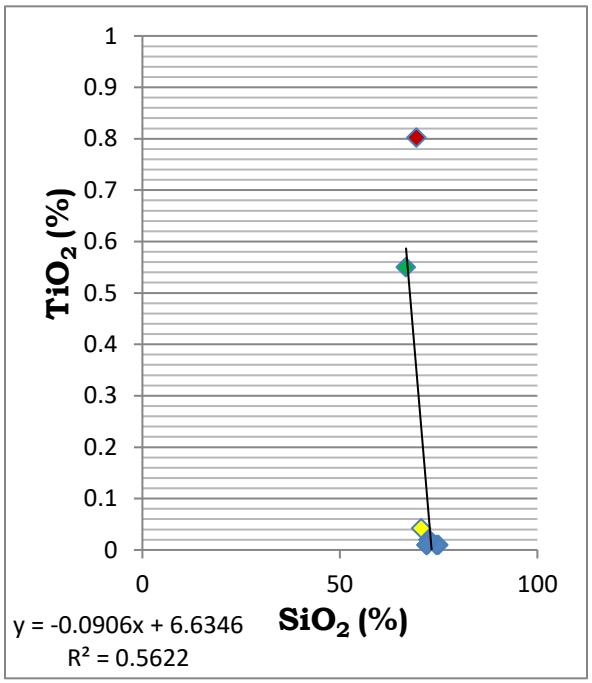

Fig 17: SiO_2 Against TiO_2

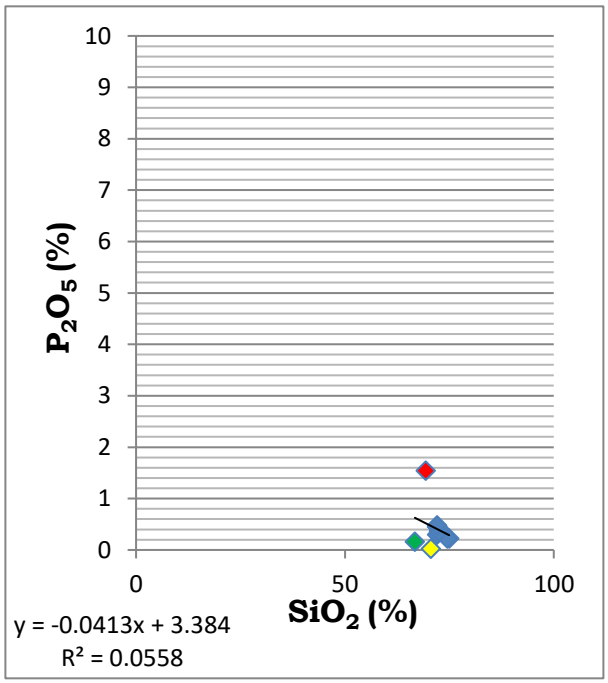

Fig 18: SiO_2 Against P_2O_5

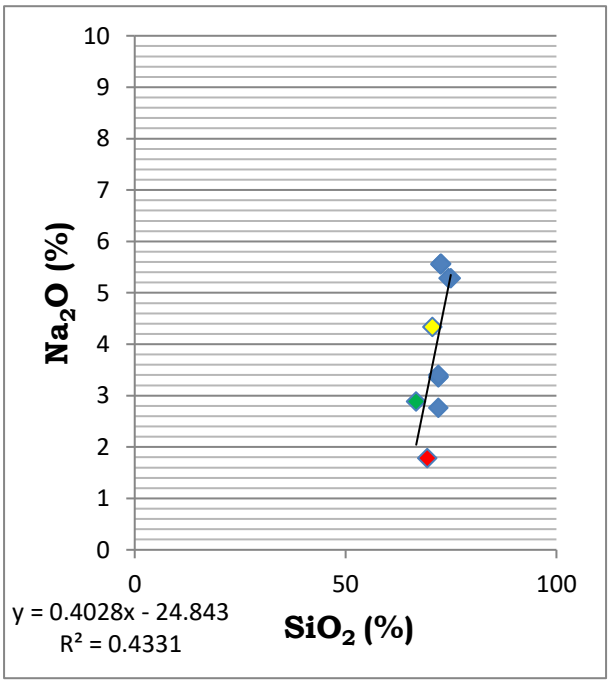

Fig 19: SiO_2 Against Na_2O

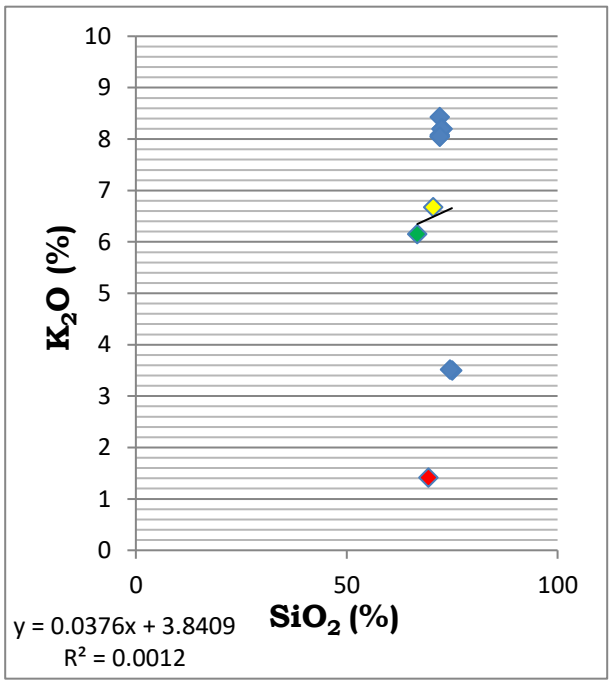

Fig 20: SiO_2 Against K_2O

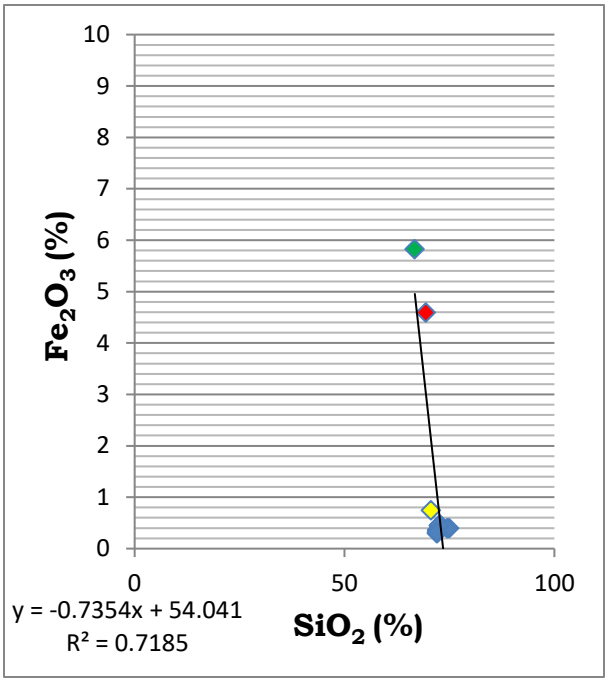

Fig 21: SiO_2 Against Fe_2O_3

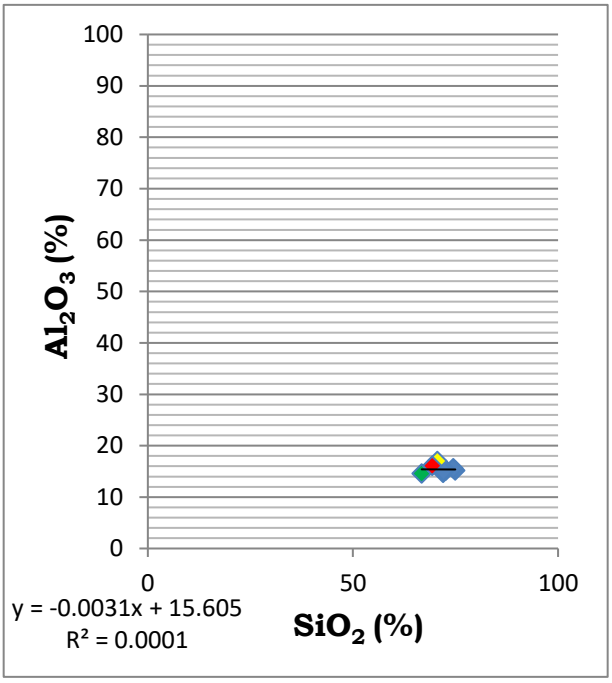

Fig 22: SiO_2 Against Al_2O_3

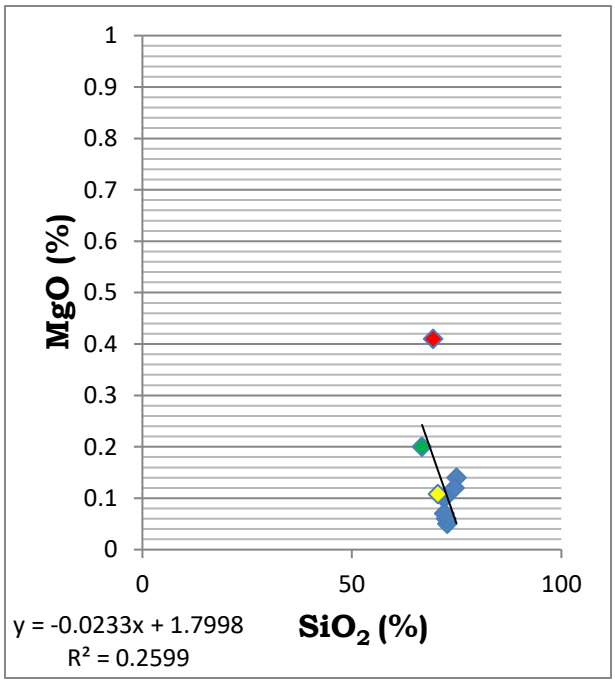

Fig 23: SiO_2 Against MgO

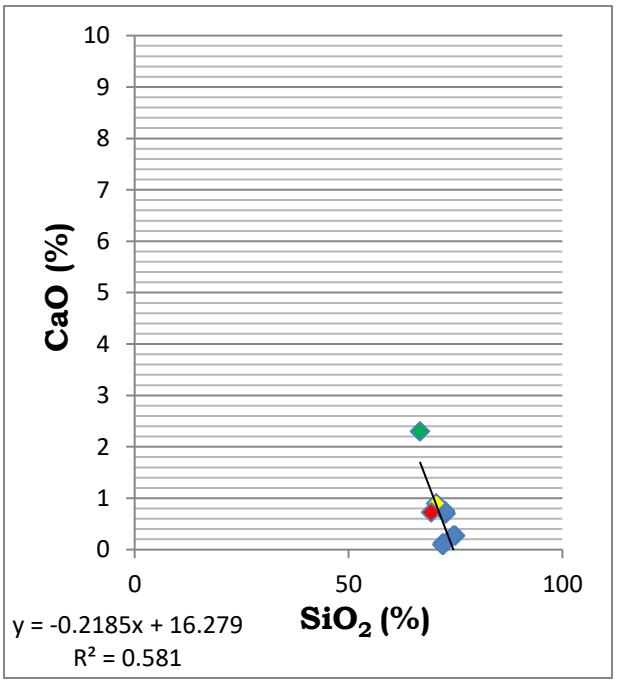

Fig 24: SiO_2 Against CaO

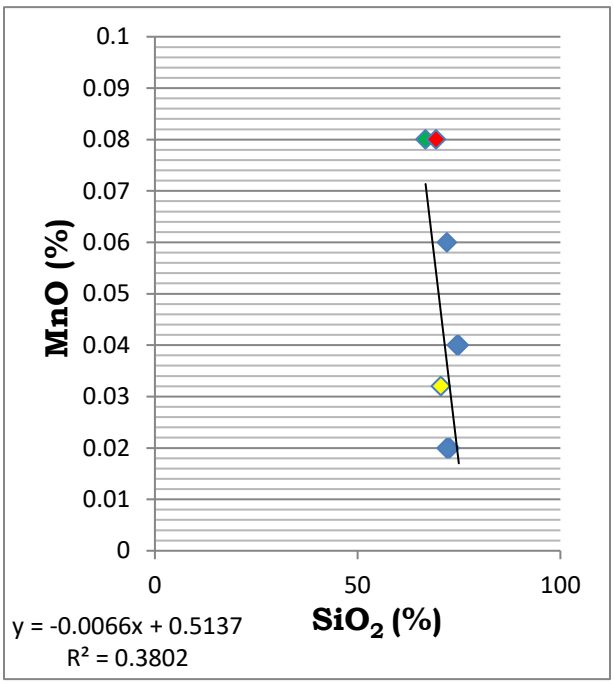

Fig 25: SiO_2 Against MnO

Legend for Bivariate Plots

LOCATION	COLOUR MARKER
DANGBALLA	BLUE
LOKOJA	YELLOW
LEMA-NDEJI	RED
HOST ROCK DANGBALLA	GREEN

BAR CHATS OF OXIDES OF DIFFERENT LOCATIONS COMPARED TO OMORUYI AND IMEOKPARIA (2021), OKUNLOLA AND AKINTOLA (2008)

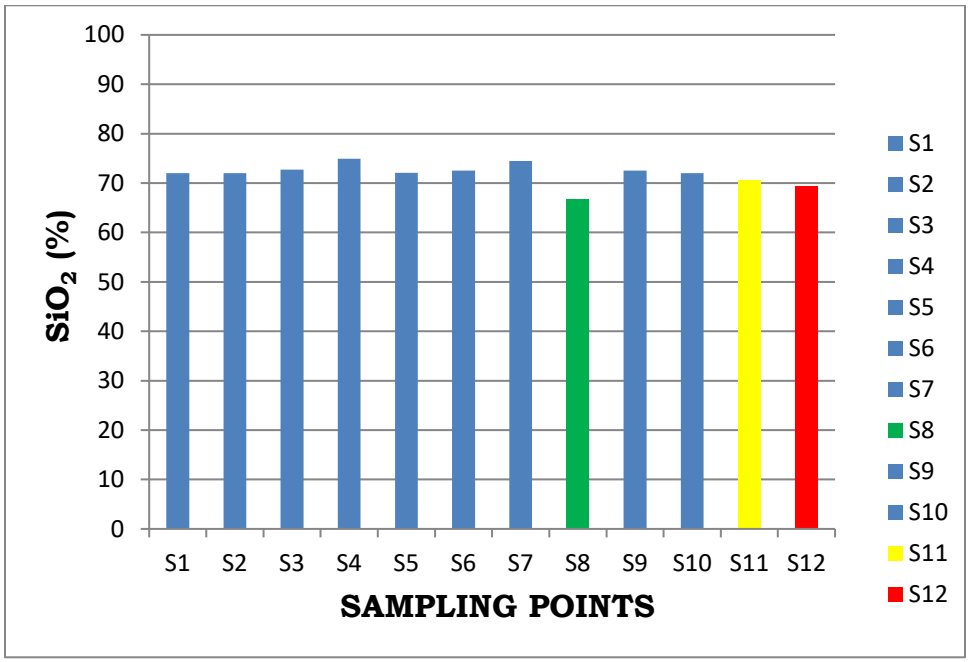

Fig 26: SiO_2 for all Sampling Points

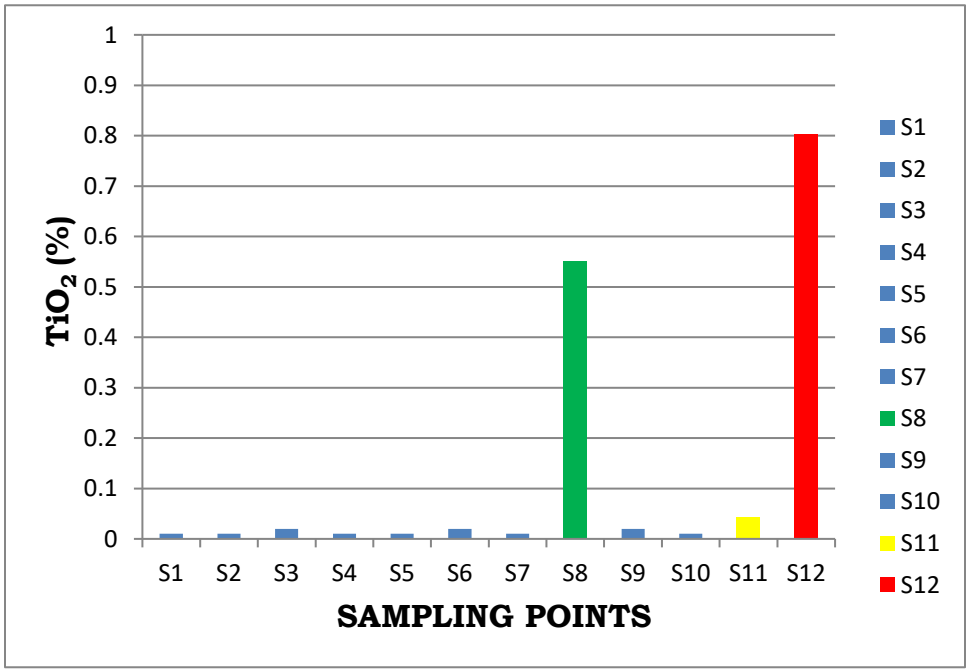

Fig 27: TiO_2 for all Sampling Points

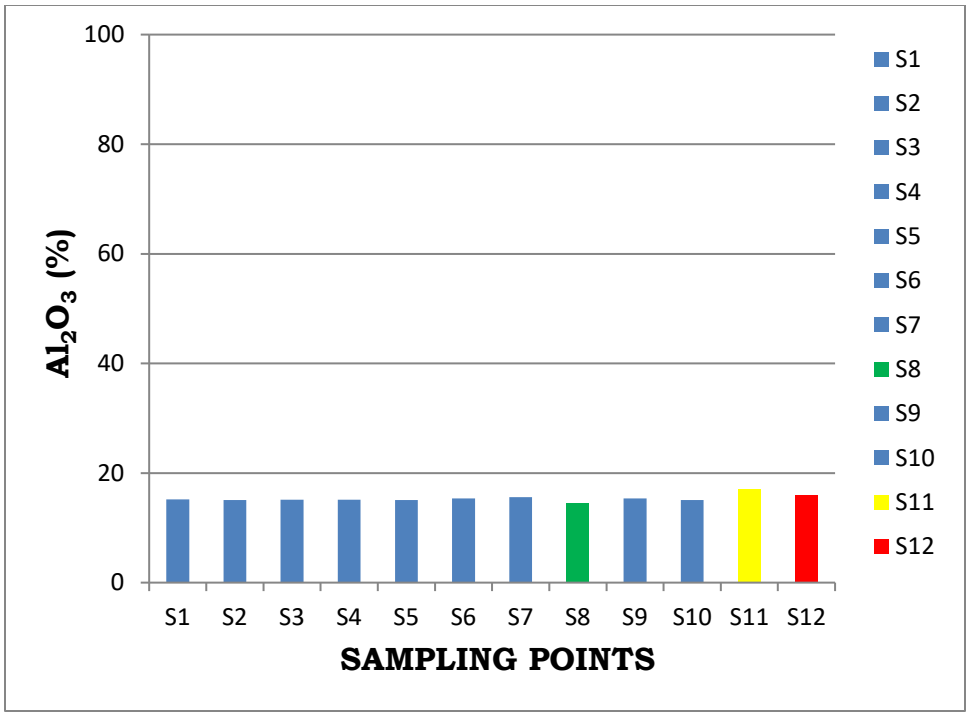

Fig 28: Al_2O_3 for all Sampling Points

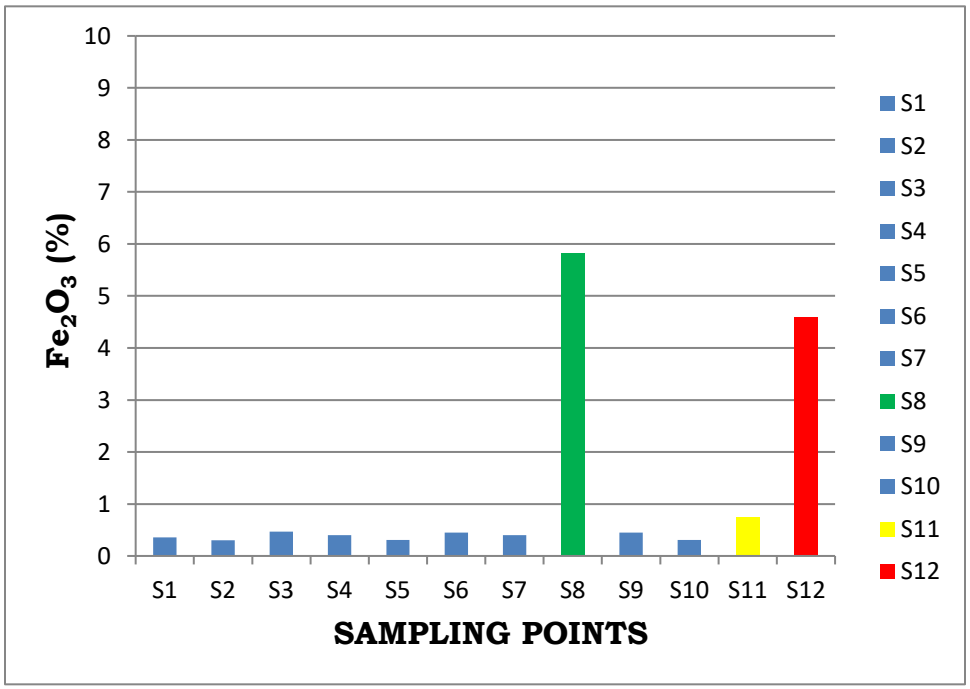

Fig 29: Fe_2O_3 for all Sampling Points

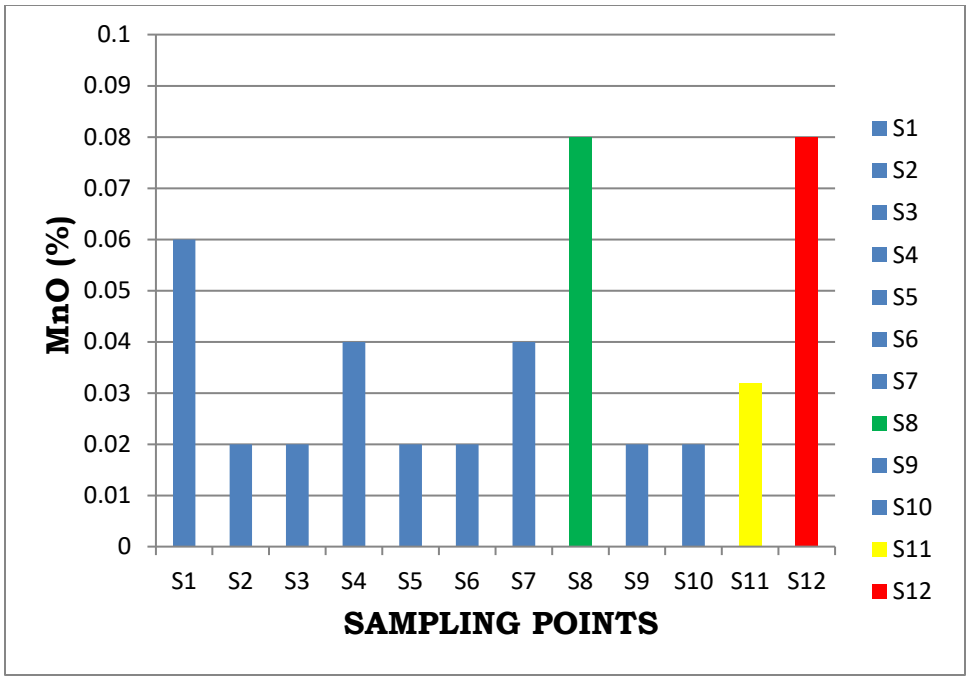

Fig 30: MnO for all Sampling Points

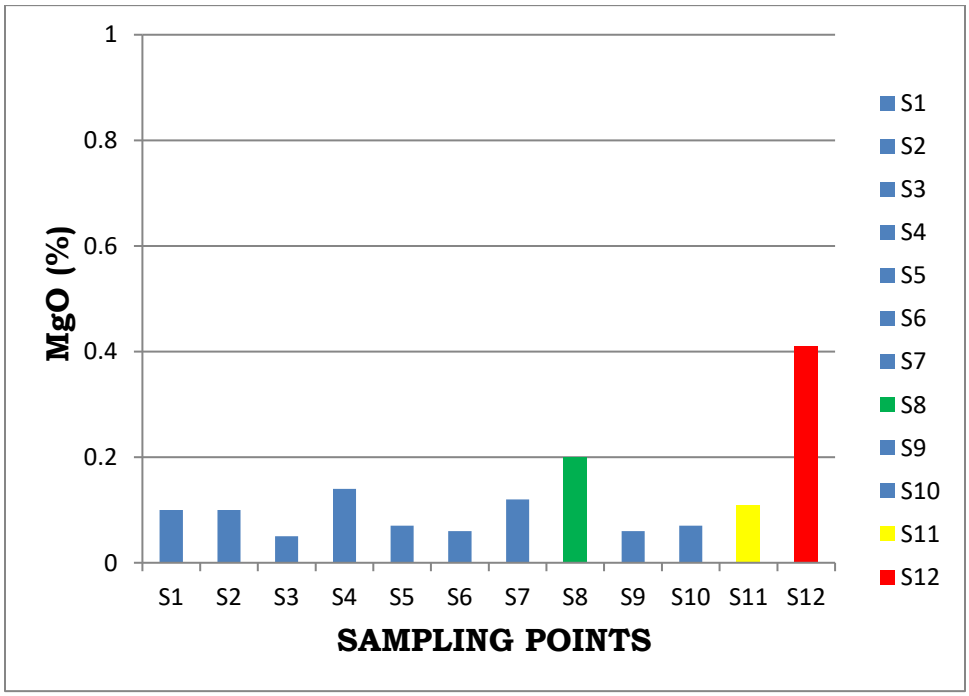

Fig 31: MgO for all Sampling Points

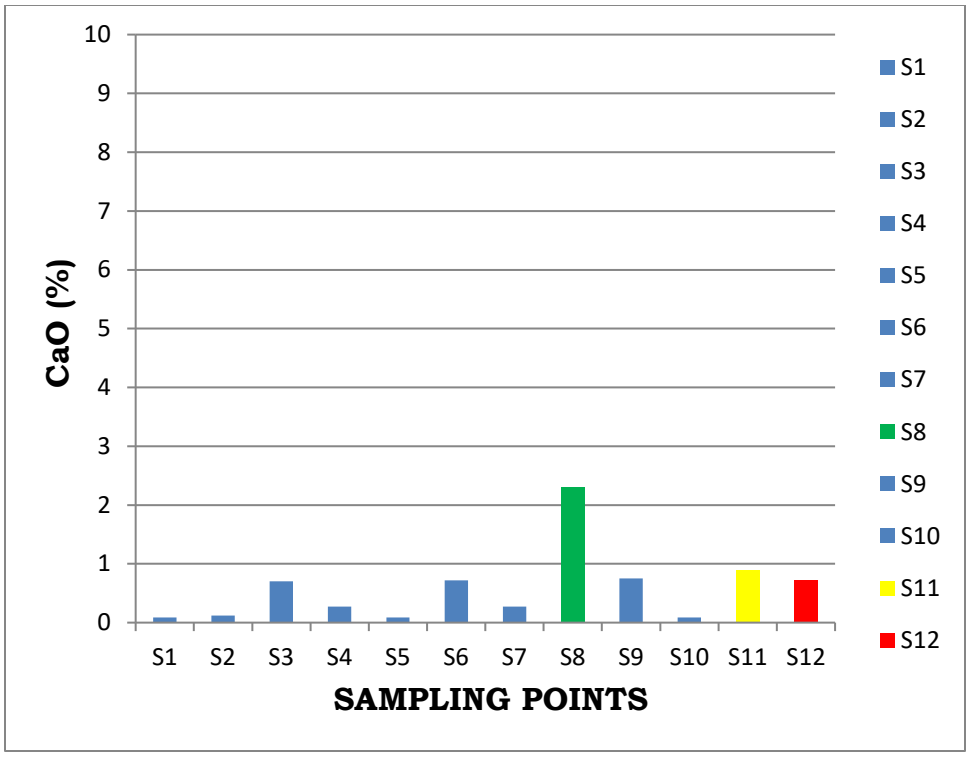

Fig 32: CaO for all Sampling Points

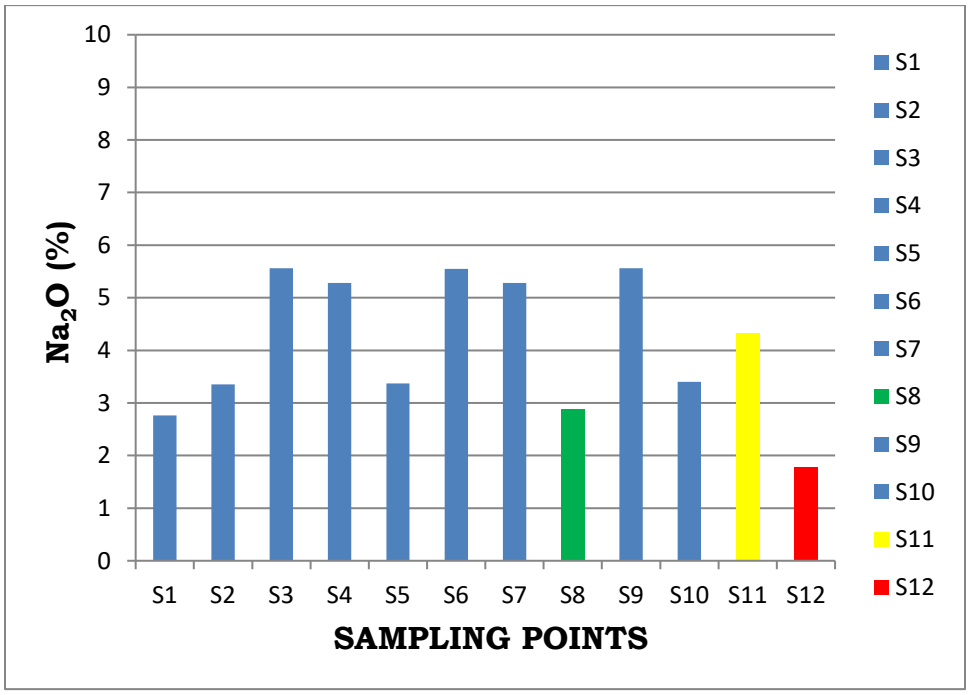

Fig 33: Na_2O for Sampling Points

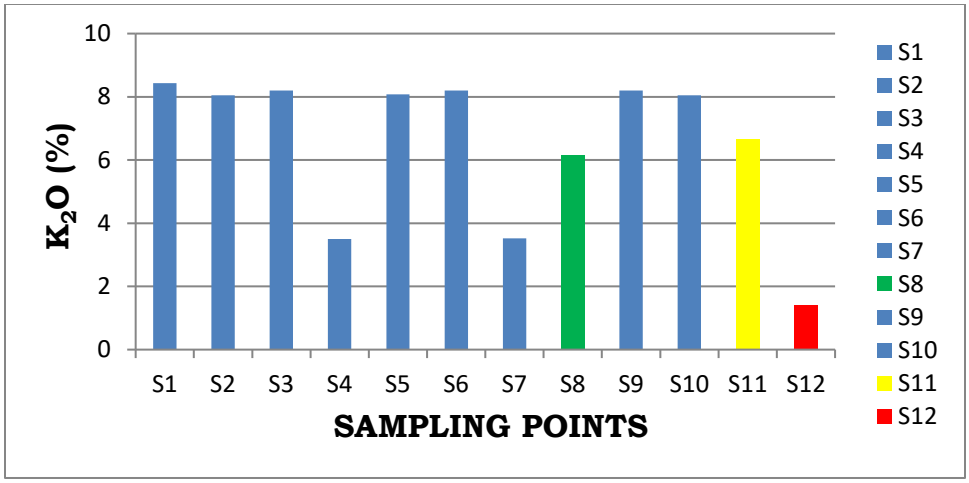

Fig 34: K_2O for all Sampling Points

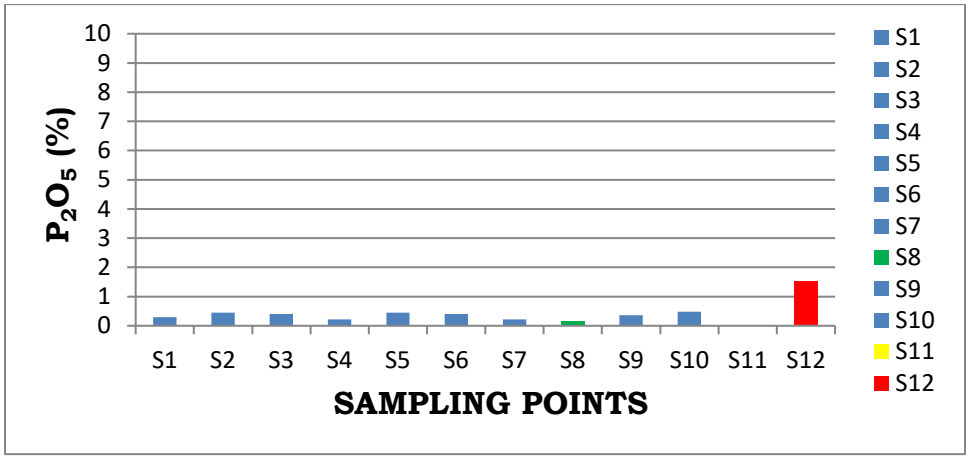

Fig 35: P_2O_5 for all Sampling Points

LEGEND FOR BAR CHARTS

LOCATION	COLOUR MARKER
DANGBALLA	BLUE
LOKOJA	YELLOW
LEMA-NDEJI	RED
HOST ROCK DANGBALLA	GREEN

Table 9: Correlation of Major Oxides in the different Rock Samples

		SiO2	TiO2	Al2O3	Fe2O3	MnO	MgO	CaO	Na2O	K2O	P2O5
SiO2	Pearson Correlation	1									
	Sig. (2-tailed)										
TiO2	Pearson Correlation	-0.879**	1								
	Sig. (2-tailed)	0.001									
Al2O3	Pearson Correlation	0.809**	-0.755*	1							
	Sig. (2-tailed)	0.005	.012								
Fe2O3	Pearson Correlation	-0.870**	1.000**	-0.747*	1						
	Sig. (2-tailed)	0.001	0.000	0.013							
MnO	Pearson Correlation	-0.561	0.754*	-0.483	0.762*	1					
	Sig. (2-tailed)	0.091	0.012	0.157	0.010						
MgO	Pearson Correlation	-0.471	0.767**	-0.531	0.773**	0.861**	1				
	Sig. (2-tailed)	0.170	.010	0.114	0.009	0.001					
CaO	Pearson Correlation	-0.785**	0.924**	-0.584	0.926**	0.595	0.576	1			
	Sig. (2-tailed)	0.007	0.000	0.077	0.000	0.070	0.081				
Na2O	Pearson Correlation	0.611	-0.388	0.648*	-0.376	-0.458	-0.373	-0.056	1		
	Sig. (2-tailed)	0.061	0.269	0.043	0.285	0.183	0.289	0.877			
K2O	Pearson Correlation	-0.318	-0.148	-0.154	-0.163	-0.370	-0.625	-0.083	-0.287	1	
	Sig. (2-tailed)	0.370	0.683	0.670	0.653	0.293	0.054	0.820	0.421		
P2O5	Pearson Correlation	0.172	-0.570	0.126	-0.585	-0.827**	-0.824**	-0.536	-0.060	0.743*	1
	Sig. (2-tailed)	0.634	0.085	0.730	0.075	0.003	0.003	0.110	0.869	0.014	
**. Correlation is significant at the 0.01 level (2-tailed).											
*. Correlation is significant at the 0.05 level (2-tailed).											

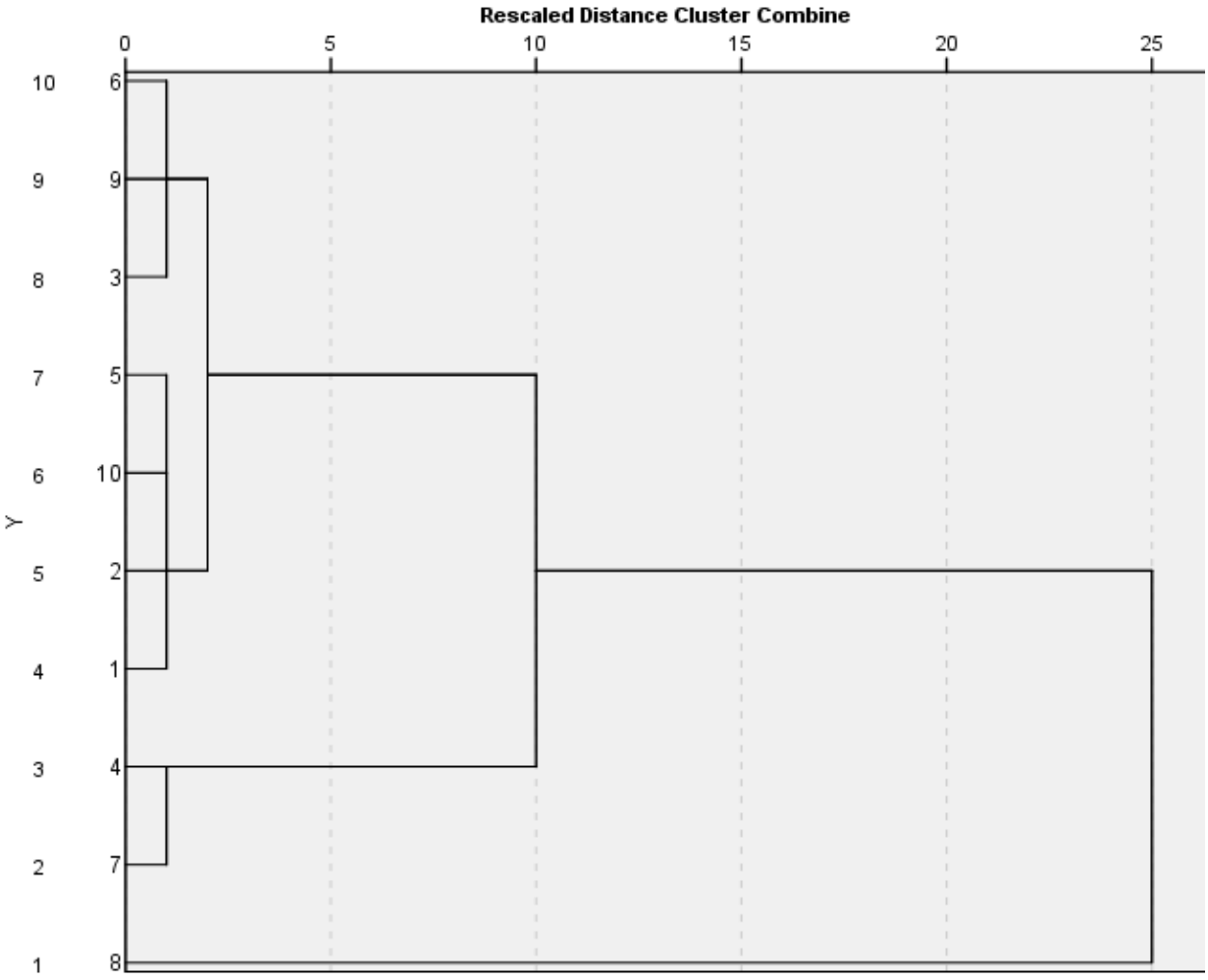

Fig 36: Dendrogram Using Average Linkage (Between Groups) Showing the Relationship between Major Oxides from 10 different Sampling Points

CHAPTER FIVE

SUMMARY, CONCLUSION AND RECOMMENDATION

5.1 SUMMARY

Results of this study show that Dagballa area is underlain mainly by Basement Rocks composed mainly of Augen-Gneiss. Intruded into this older lithology are Pegmatite Dykes. These Pegmatite bodies are extensive and cover a substantial area of Dagballa. They are mineralogically composed mainly of quartz, microcline, albite and the micas. Microcline is the major feldspar mineral present in the samples with compositions ranging between 30-80%; they likely indicate granite origin. It is colorless and cloudy, showing alterations to sericite. It is recognized by its characteristic grid (cross-hatched) twinning under crossed-polarized light. It also occurs as anhedral-subhedral crystals with low relief and it exhibits no pleochroism.

The results of the analyses show that the composition of the major oxides obtained from Dagballa, relates closely with the mean compositions of the oxides obtained from Lokoja Area. This probably suggests that feldspar present in Pegmatite rocks in the same area are of identical origin. The composition of the major oxides obtained from the host rock in Dagballa relates closely with the mean compositions obtained from Lema-Ndeji with the exception of Al_2O_3, CaO, K_2O and P_2O_5. This similarity could probably be linked to the Granite Gneiss which is the host rock present in both areas.

The association of silica (SiO_2) with other with other major oxides analyzed in this study shows a significant correlation positively with phosphate (P_2O_5) and soda (Na_2O) with correlation coefficient of 0.0296 and 0.3708 respectively. Silica (SiO_2) shows a significant correlation negatively with TiO_2, K_2O, Fe_2O_3, Al_2O_3, MgO, CaO and MnO with correlation coefficient of 0.772, 0.1013, 0.757, 0.6539, 0.2217, 0.616 and 0.3149 respectively. When compared with the mean values obtained from Lokoja and Lema-Ndeji, only Na_2O with a correlation coefficient of 0.4331 showed a positive correlation relationship with SiO_2. The other oxides show a negative correlation relationship with SiO_2 when compared with the mean values obtained from Lokoja and Lema-Ndeji.

Test of significance of observed correlation coefficients showed there were 45 correlations between the major oxides and 13 were found to have significance at 1% ($P<0.01$) level.

The rock samples from Alumina Saturation Index computation shows that the rock samples present in the Dagballa area are peraluminous.

5.2 CONCLUSION

The results obtained from thin section study shows that the main components of the rock samples are quartz, feldspar (microcline and albite), mica and some opaque minerals. This class of mineral assemblage indicates emplacement in continental environment.

XRF data obtained from the pegmatite samples in Dagballa compares favorably with the mean values from the pegmatite samples in Lokoja, which shows the samples in both locations have similar major and minor oxides compositions.

Analysis from bivariate plot, regression and dendogram shows that soda (Na_2O) shows a strong relationship with the other major oxides present. This oxide is a major constituent of albite and it is present in substantial quantities in microcline and these minerals are major component parts of all the rock samples.

5.3 RECOMMENDATION

The pegmatite and augen-gneiss present in the area can serve as source of income and job creation when exploited properly. There is a lot of illegal mining going on in one of the locations visited; government should put proper machinery in place to curb this menace. The study area is characterized by many different types of trees which if the habit of afforestation is employed, the trees could serve as source of domestic fuel and construction works. The government and local authority should also try to stop indiscriminate hunting and cutting down of trees in the study area to preserve the forestry. Hydrogeological investigation using geophysical survey method should be employed to boost productivity of water in the study area hence it will help to improve the water problems in the area both for domestic and for irrigation purpose.

APPENDIX

RESULTS OF LABORATORY AND GEOCHEMICAL ANALYSIS

Table 10: Trace Element Compositions from XRF Analysis

S/No	Element	Certified	Measurement	Anode
1	Ba	19650 (350)	14040 (750)	Rh
2	Cs	415 (25)	450 (55)	W
3	Rb	310 (25)	408 (50)	W
4	Ta	1885 (55)	730 (38)	W
5	Sr	135 (12)	145 (20)	Rh
6	Nb	68 (6)	58 (21)	W

Table 11: Mass of element (ug) measured in standard reference material (SRM) 2785 and X-ray tube used in the measurement

Element	Ba	Cu	Pb	Ni	Cr	Ce	Rb	Zr
Average	55.0	0.5	0.2	0.1	12.0	2.5	6.3	4.0
Std.dev	0.78	0.02	0.01	0.01	0.02	0.02	0.02	0.01
Exp.value	450.1	33.3	10.1	34.2	99.02	55.0	96.1	68.0

References

Ademila, O., Okpoli, C.C., Ehinmitan, D., (2019). Geological and Lithological Mapping of Part of Igarra Schist Belt Using Integrated Geophysical Methods. Earth Sciences Pakistan (ESP).

Ajibade, A.C., Woakes, M., Rahaman, M.A., (1987). Proterozoic crustal development in the Pan African regime of Nigeria, In: Proterozoic lithospheric evolution. American Geophysical Union, Special Publication (Edited by Kroner, A.), pp 259-271.

Ajibade, A.C., & Wright, J.B., (1989). The Togo-Benin, Nigeria shieldevidence of crustal aggregation in Pan African belt. Tectonophysics, 155.

Akande, A.O., & Kinnaird, J., (1990). Characterization and origin of ore-forming fluids in the Nigerian mineral belts. Proceedings of the Eight Quadrennial IAGOD Sumposium, Ottawa, Canada, pp 199-218.

Akintola, O.F., and Adekeye, J.I., (2008). Mineralization controls and petrogenesis of rare pegmatites of Nasarawa area, Central Nigeria. Earth Science Res. Journal, Vol. 12 (1). Pp. 1-11.

Annor, A.E., (1998). Structural and Chronological relationship between the low-grade Igarra Schist and its adjoining Okene Migmatite-Gneiss terrain in the Precambrian exposure of Southwestern Nigeria. J.Min. Geol. 34 (2): 187-196.

Ayodele, S.O., (2015). The geology, geochemistry and petrogenetic studies of the Precambrian Basement rocks around Iworoko, Are and Afao area, Southwestern Nigeria. Journal of Environment and Earth Science. 5(3): 58-66.

Ball, E., (1980). An example of very consistent brittle deformation over a wide intercontinental area: The late Pan-African fracture system of the Taureg and Nigeria shield. Tectonophysics. 61(4). Pp. 363-379.

Bankole, S., (2016). Hydrocarbon potential of Post Santonian sediments in Anambra Basin, Southeastern Nigeria.

Boesse, S. and Ocan, O., (1992). Geology and evolution of the Ife-Ilesha Schist belt, southwestern Nigeria, In Benin-Nigeria Geotraverse, International Meeting on the Proterozoic Geology and Tectonics of High Grade Terrain, IGCP 215, 123-129.

Bucher, K., & Grapes, R. (2011). Petrogenesis of metamorphic rocks. Springer Science 7 Business Media.

Cerny, P., (1989). Characteristics of pegmatite deposits of Tantalu. In MOLLER, P., CERNY, P., and SAUPPE, F., (eds) Lanthanides, tantalum and niobium: Springer Verlag, Berlin 145-154.

Cerny, P., London, D., and Novak, M., (2012). Granitic pegmatites as reflections of their sources. Elements 8: 289-294.

Dada, S.S., (1997). Proterozoic evolution of the Nigeria-Boborema province.

Dada, S.S., (1998). Crust-Forming ages and Proterozoic Crustal Evolution of Nigeria: A Reappraisal of Current Interpretations. Precambrian Research 87 (1-2), 65-74.

Dada, S.SS, (2006). Proterozoic evolution of Nigeria. In: Oshi O (ed) The Basement Complex of Nigeria and its mineral resources (A Tribute to Prof. M.A.O. Rahaman), Akin Jinad and Co. Ibadan, pp 29-44.

Danbatta, U.A., (2003). The tectonic significance of the NNE-continuation of the Kalangai fault zone into Kazuare Schist Belt of NW Nigeria. Science Africana, Vol. 2 (1 and 2), pp. 17-25.

Dyar, M.D. and Gunter, M.E., (2008). Mineralogy and Optical Mineralogy. Mineralogical Society of America.

Egbuniwe, I.G., (1982). Geotectonic evolution of the Maru Belt, NW Nigeria. Unpublished Ph.D. Thesis, University of Wales, Aberystwyth.

Falconer, J.D., (1911). The Geology and Geography of Northern Nigeria. London, Macmillan. Pp. 135-146.

Frost, B.R., Frost, C.D, (2008). A geochemical classification for feldspathic Igneous rocks. Journal of Petrology, v. 49, p. 1955-1969.

Garba, I., (2003).Geochemical discrimination of newly discovered rare-metal bearing and barren pegmatites in the Pan-African (600± 150 Ma) Basement of Northern Nigeria. Applied Earth Science (Trans. Inst. Min. Metall. B) 112, B287.

Hobart, M.K., (2015). Pegmatite: An extreme igneous rock with large crystals and rare minerals.

Hobart, M.K., (2015). Feldspar: A large group of silicate minerals.

Imasuen, O.I., Olatunji, J.A., and Oyeobi, T.U.S., (2013). Geological Observation of Basement rocks around Gangu, Kogi State. International Research Journal of Geology and Mining, 3(2): 57.

Imeokparia, E.G., and Emofurieta, W.O., (1991). Protoliths and petrogenesis. Journ., Chem. Erde51, 337-347.

Jacobson, R.E.E., Webb, J.S., (1946). The pegmatites of Central Nigeria. Geological Survey of Nigeria Bulletin 17, 1-73.

Kuster, D., (1990). Rare metal pegmatites of Wamba: Central Nigeria their formation in relationship to Late Pan-African Granite. J. Mineral Deposits 25: 25-33.

London, D., Kontak, D.J., (2012). Elements; An international Magazine of Mineralogy, Geochemistry, and Petrology.

McCurry, P., (1976).The Geology of the Precambrian to lower Paleozoic rocks of Nigeria. In: Kogbe, C.A., (ed) Geology of Nigeria. Elizaberthan, Lagos Nigeria, 15-31.

McCurry, P., (1989). A general review of the geology of the Precambrian to Lower Paleozoic rocks of Northern Nigeria. In: Kogbe, C.A. (Ed.), Geology of Nigeria, Rock View, Jos, 13-37.

McNamee, B.D., and Gunter, M.E., (2014). Mineralogy and Optical Mineralogy Lab Manual.

Muhammad, A.U., (2014). Geology and Geochemistry of rocks and Banded Iron Formation of Northern Part of Wonaka Schist Belt, Northwestern Nigeria.

Nigerian Geological Survey Agency (2015).

Obiadi, I.I., Obiadi, C.M., Ajaegwu, N.E., Anakwuba, E.K., Onuigbo, N.E., Maduewesi, U.V., Okolo, and C.M., Ezim, O.E., (2015). Structural Evidence for Pan-African Event in the SW Basement Block of Nigeria: The Igarra Example. Journal of Basic and Applied Research International, 65-74.

Odeyemi, I.B., (1976). Preliminary report on the field relationships of Basement Complex rocks around Igarra, Mid-Western State, Nigeria: Geology of Nigeria, University of Ife, Nigeria.

Odeyemi, I.B., (1988). Lithostratigraphy and structural relationships of the Upper Precambrian Metasediments in Igarra area, Southwestern Nigeria.

Ogbe, O.B., Olobaniyi, S.B., Ejeh, O.I., Omo-Irabor, O.O., Osokpor, J., Ocheli, A., & Oveare, B., (2018). Petrological and Structural Investigation of Rocks around Igarra, Southwestern Nigeria. Ife Journal of Science vol. 20, no 3 (2018), 663-677.

Ogezi, A.E.O., (1977). Geochemistry and geochronology of Basement rocks from NW Nigeria. Ph.D. Thesis, Leeds University.

Okeke, P.O. and Meju, M.A., (1985). Chemical evidence for the sedimentary origin supracrustal rocks, Southwest, Nigeria.

Okunlola, O.A., (2005). Metallogeny of Tantalum-Niobium mineralization of Precambrian pegmatites of Nigeria. Mineral wealth. Athens Greece 183/2005 p 30-35.

Okunlola, O.A., & Akintola, A.I., (2008). Compositional features and rare metal (Ta-Nb) potentials of Precambrian pegmatites of Lema-Ndeji area, Central Nigeria. Mineral Wealth 149, 43-53.

Okunlola, O.A., & Somorin, E.B., (2006). Composition features of Precambrian Pegmatites of Itakpe Area, Central Nigeria. Global Journal of Geophysical Sciences 4 (2), 221-230.

Olobaniyi, S.B., (2003). Geochemistry of Semi-pelitic Schist of Isanlu Area, S.W. Nigeria: Implication for the geodynamic evolution of the Egbe-Isanlu Schist belt. Global journ. Geological Science 1(2), 113-127.

Oloto, I.N., & Anyanwu, DD.E, (2013). Petrology of Ibillo-Mangongo Area of Igarra, Edo State Nigeria. Pelagia Research Library, 140-145.

Omoruyi, D.I., Imeokparia, E.G., (2021).Geochemical Characterization and Rare-Metals (Ta-Nb) Mineralization Potentials of Pegmatites Around Lokoja, Central Nigeria. International Journal of Earth Sciences Knowledge and Applications, 69-77.

Oyewole, A.M., Ofuyah, W.N., (2017). The Geology of Eshiawa in Igarra Area, Southwestern Nigeria.

Rahaman, M.A., (1981). Recent advances in the study of the Basement Complex of Nigeria. Abstract, 1st Symposium on the Precambrian Geology of Nigeria.

Rahaman, M.A., (1988). Recent advances in the study of the Basement Complex of Nigeria. In: Oluyide, P.O., Mbonu, W.C., Ogezi, A.E., Egbuniwe, I.G., Ajibade, A.C. and Umeji, A.C., (eds). Precambrian Geology of Nigeria, Geological Survey of Nigeria, 11-43.

Rollinson, H.R., (1993). Using Geochemical Data: Evaluation, Presentation, Interpretation.

Shelley, D. (1993). Igneous and metamorphic rocks under the microscope: classification, textures, microstructures and mineral preferred-orientations.

Shugar, A., (2009). An introductory explanation of how to interprete XRF data.

Suleiman, A.B., (2016). The Geology of Butawa, Kafin Magaji and their environs, part of sheet 79 (Mulumfashi) NE.

Turner, D.C., (1983). Upper Proterozoic Schist Belts in the Nigerian sector of the Pan African Province of West Africa. Precambrian Resources 21, pp. 5-79.

Turpin, B.J., Cary, R.A., and Huntzicher, J.J., (1990). An in-situ time resolved analyzer for aerosol organic and elemental carbon. Aerosol Sci. Technol. 12 (1): 161-171.

Williams, H., Turner, & F.J., Gilbert, C.M., (1982). An Introduction to the study of Rocks in Thin Section.

Winter, J.D., (2014). Principles of Igneous and Metamorphic Petrology.

Vernon, R.H. & Clarke, G.L. (2008). Principles of Metamorphic Petrology. Cambridge university press.

Vernon. R.H. (2018). A practical guide to rock microstructure. Cambridge university press.